NASA TN D-306

TN-34
198714
P71

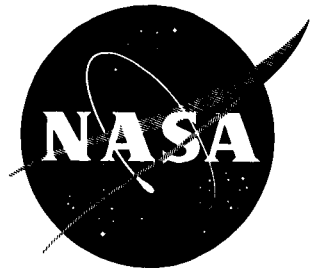

TECHNICAL NOTE
D-306

A SIMPLIFIED STUDY ON THE NONEQUILIBRIUM COUETTE AND BOUNDARY-LAYER FLOWS WITH AIR INJECTION

By Paul M. Chung

Ames Research Center
Moffett Field, Calif.

NATIONAL AERONAUTICS AND SPACE ADMINISTRATION

WASHINGTON February 1960

(NASA-TN-D-306) A SIMPLIFIED STUDY ON THE NONEQUILIBRIUM COUETTE AND BOUNDARY-LAYER FLOWS WITH AIR INJECTION (NASA. Ames Research Center) 71 p

N89-70943

Unclas
00/34 0198714

1H

NATIONAL AERONAUTICS AND SPACE ADMINISTRATION

TECHNICAL NOTE D-306

A SIMPLIFIED STUDY ON THE NONEQUILIBRIUM COUETTE AND BOUNDARY-LAYER FLOWS WITH AIR INJECTION

By Paul M. Chung

SUMMARY

A theoretical study was made on the simultaneous effect of the finite rate of recombination of oxygen atoms and the fluid injection on the heat transfer to a flat surface.

The Couette flow model was analyzed first, and then the steady laminar boundary layer over a flat plate was studied by Rayleigh's analogy.

The following two major approximations were made in order to obtain some qualitative information on the subject without excessive numerical calculations.

1. All the property values except temperature and atom mass fraction were considered to be constant.

2. A special linear approximation of the homogeneous reaction rate law was employed.

It was found that the surface catalytic recombination is more important than the gas-phase recombination, when they are of the same order of magnitude, as far as their effects on the heat transfer is concerned.

For a boundary layer developing from the leading edge of a finite plate, the effect of the gas-phase recombination is to increase the heat transfer to the plate about one-third of the way, at the most, toward the equilibrium value from the frozen case. The calculation was based on the condition of air at the edge of the boundary layer approximately corresponding to that at a flat afterbody of a blunt nosed hypersonic vehicle.

The Couette flow analysis showed that the major role of the fluid injection is to shield the surface from the conduction of the sensible heat and from the diffusion of the atoms to the surface rather than to affect the chemical reactions except when the specific reaction rates are sufficiently low.

The injection of fluid into a boundary layer was found to decrease the effect of the gas-phase reaction on the heat transfer for a given relaxation time and for a given position along the surface.

INTRODUCTION

The air surrounding a vehicle in hypersonic flight usually contains a considerable amount of dissociated radicals which are created by the strong shock preceding the vehicle or by the extremely high friction in the boundary layer. These radicals recombine as they flow along the surface of the vehicle. The recombination may occur in the inviscid stream, in the boundary layer, or at the surface of the vehicle. Any one of these recombination phenomena can cause a considerable variation in the heat transfer to the vehicle.

Much study has been carried out on the subject of fluid mechanics with dissociation and recombination phenomena and a rather complete resumé of the work appears in reference 1.

A
3
3
6

In most of the previous studies, the processes of dissociation and recombination were considered to occur at an extremely fast rate, so that the air was locally in an equilibrium state. Such a consideration simplifies the work greatly. It is known, however, that the chemical reactions of dissociation and recombination occur at the extremely fast rate only for a very limited range of flight conditions and locations along the surface. The reactions more likely take place at a finite rate and the air is in a nonequilibrium state.

In high-speed flight, some form of mass injection cooling of the boundary layer has been generally recognized as an effective and a practical method of protecting the vehicle from the surrounding high-energy gas. The problem of fluid injection into a chemically inert boundary layer has been studied rather thoroughly. The problem of fluid injection into a boundary layer which is chemically reacting at a finite rate has not previously been studied.

The major obstacle to the theoretical study of the nonequilibrium, chemically reacting boundary layer lies in the extremely complicated nature of the equations which describe such phenomena.

It is the main object of the present study to gain qualitative information on the combined effect of nonequilibrium dissociation, recombination, and air injection for a laminar boundary layer.

The Couette flow model is considered first. The steady boundary-layer flow on a flat plate is then studied by Rayleigh's analogy. During the course of the analysis, the appropriate equations are simplified, by a series of approximations, so that they could be solved without excessive numerical work.

SYMBOLS

C	number of oxygen atoms, free or combined, per unit mass of fluid
c_p	constant pressure specific heat of mixture
c_{p_i}	constant pressure specific heat of ith species
D	binary diffusion coefficient
E	Eckert number, $\frac{u_\infty^2}{c_p(T_\infty - T_w)}$
$\operatorname{erf} x$	$\frac{2}{\sqrt{\pi}} \int_0^x e^{-z^2} dz$
h	enthalpy defined by equations (5) and (6a)
Δh^o	heat of dissociation of oxygen measured at a reference temperature
K_e	equilibrium constant
k_D	specific rate constant for dissociation
k_R	specific rate constant for recombination
k_w	specific rate constant for catalytic surface recombination
L	distance between two plates in Couette flow
Le	Lewis number, $\frac{Pr}{Sc}$
m	$\frac{m_A}{m_{A,\infty}}$
m_A	fraction of total oxygen atoms in atomic form
N_A	number of atoms produced per unit volume per unit time
n	mass per oxygen atom
Nu	Nusselt number based on x, $\frac{qx}{\lambda(T_\infty - T_w)}$
Nu_L	Nusselt number based on L, $\frac{qL}{\lambda(T_\infty - T_w)}$

A 3 3 6

O	number density of oxygen atoms
O_2	number density of oxygen molecules
P	total number density in the mixture
Pr	Prandtl number, $\frac{\mu c_p}{\lambda}$
Pr_e	effective Prandtl number defined by equation (47b)
p	pressure
q	total heat transfer to the wall
Re	Reynolds number, $\frac{u_\infty x}{\nu}$
r	independent variable used in equation (B1)
Sc	Schmidt number, $\frac{\mu}{\rho D}$
T	absolute temperature
t	time
U	dimensionless x component of velocity, $\frac{u}{u_\infty}$
u	x component of velocity
v	y component of velocity
v_o	constant for fluid injection parameter
W_i	net mass production rate of ith species per unit volume
X_i	mass fraction of ith species
x	direction and distance along surface
Y	$\frac{y}{L}$
y	direction and distance normal to surface
z	dummy variable of integration
γ_w	dimensionless parameter for catalytic surface reaction, $\frac{L\rho k_w}{\mu}$
δ	dimensionless parameter for fluid injection, $\frac{\rho v_w L}{\mu}$

A
3
3
6

η dimensionless similarity ordinate defined by equation (56)

θ dimensionless temperature, $\frac{T - T_w}{T_\infty - T_w}$

λ thermal conductivity of gas

μ absolute viscosity of gas

ν kinematic viscosity of gas, $\frac{\mu}{\rho}$

ξ ratio of characteristic flow time to relaxation time, $\frac{t}{\tau}$

ρ density of gas

τ relaxation time defined by equation (15)

$\frac{1}{\tau_1}$ specific homogeneous reaction rate for Couette flow, $\frac{L^2}{D}\left(\frac{1}{\tau}\right)$

$\frac{1}{\tau_2}$ $\frac{L^2 \Delta h^o X_{A,\infty}}{\lambda(T_\infty - T_w)}\left(\frac{\rho}{\tau}\right)$

Superscript

$'$ total differentiation with respect to Y in Couette flow and with respect to η in boundary-layer flow

Subscripts

A oxygen atoms

e equilibrium state

i ith species

M molecules

w at the wall (stationary plate in case of Couette flow)

∞ at moving plate in case of Couette flow, and at outer edge of boundary layer in case of boundary-layer flow

BASIC CONSERVATION EQUATIONS

Air in the present analysis is assumed to be comprised of molecular oxygen, nitrogen, and atomic oxygen. The only chemical reaction considered is the dissociation and recombination of oxygen in the air.

The following equations describe the behavior of the air in a two-dimensional laminar boundary layer.

$$\frac{\partial \rho}{\partial t} + \frac{\partial \rho u}{\partial x} + \frac{\partial \rho v}{\partial y} = 0 \qquad \text{continuity} \tag{1}$$

$$\rho\left(\frac{\partial u}{\partial t} + u\,\frac{\partial u}{\partial x} + v\,\frac{\partial u}{\partial y}\right) = \frac{\partial}{\partial y}\left(\mu\,\frac{\partial u}{\partial y}\right) \qquad \text{momentum} \tag{2}$$

$$\rho\left(\frac{\partial h}{\partial t} + u\,\frac{\partial h}{\partial x} + v\,\frac{\partial h}{\partial y}\right) = \frac{\partial}{\partial y}\left(\lambda\,\frac{\partial T}{\partial y} + \rho D\sum_i h_i\,\frac{\partial X_i}{\partial y}\right) + \mu\left(\frac{\partial u}{\partial y}\right)^2 \qquad \text{energy} \tag{3}$$

$$\rho\left(\frac{\partial X_i}{\partial t} + u\,\frac{\partial X_i}{\partial x} + v\,\frac{\partial X_i}{\partial y}\right) = \frac{\partial}{\partial y}\left(\rho D\,\frac{\partial X_i}{\partial y}\right) + W_i \qquad \text{diffusion} \tag{4}$$

where

$$h = \sum_i X_i h_i \tag{5}$$

It is assumed in the above equations that the pressure gradient is zero. The particular form of diffusion equation used here is strictly correct only for a binary mixture of gases. The three constituents involved here, however, are mechanically sufficiently similar so that the diffusion equation (4) is thought to be applicable to the present case. The term W_i in equation (4) represents the net production rate of the ith species by the chemical reaction per unit volume. Usually W_i is expressible as an explicit function of temperature, pressure, and mass fractions of the species. Here it is more convenient, therefore, to have an energy equation in terms of temperatures rather than enthalpies.

In equation (5)

$$h_i = \int_{T_o}^{T} c_{p_i}\,dT + h_i^o \tag{6a}$$

where h_i^o is the heat of formation of the ith species measured at the reference temperature, T_o.

From equation (5)

$$dh = \sum_i X_i dh_i + \sum_i h_i dX_i \tag{6b}$$

and from equation (6a)

$$dh_i = \left(\frac{\partial h_i}{\partial T}\right) dT = c_{p_i} dT$$

Therefore, equation (6b) becomes

$$dh = c_p dT + \sum_i h_i dX_i \tag{7}$$

where

$$c_p = \sum_i X_i c_{p_i}$$

The relationship (7) changes equation (3) to the following form

$$\rho c_p\left(\frac{\partial T}{\partial t} + u\,\frac{\partial T}{\partial x} + v\,\frac{\partial T}{\partial y}\right)$$
$$= \frac{\partial}{\partial y}\left(\lambda\,\frac{\partial T}{\partial y}\right) + \mu\left(\frac{\partial u}{\partial y}\right)^2 - \sum_i\left[h_i\left(\rho\,\frac{\partial X_i}{\partial t} + \rho u\,\frac{\partial X_i}{\partial x} + \rho v\,\frac{\partial X_i}{\partial y}\right) - \frac{\partial}{\partial y}\left(\rho D h_i\,\frac{\partial X_i}{\partial y}\right)\right]$$

This becomes, with the aid of equation (4),

$$\rho c_p\left(\frac{\partial T}{\partial t} + u\,\frac{\partial T}{\partial x} + v\,\frac{\partial T}{\partial y}\right) = \frac{\partial}{\partial y}\left(\lambda\,\frac{\partial T}{\partial y}\right) + \mu\left(\frac{\partial u}{\partial y}\right)^2 - \sum_i\left[h_i W_i - \rho D\left(\frac{\partial X_i}{\partial y}\right)\left(\frac{\partial h_i}{\partial y}\right)\right] \tag{8}$$

Now, in equation (8),

$$W_M = -W_A$$

and

$$\sum_i h_i W_i = \left(h_A - h_M\right) W_A$$

with the aid of equation (6a), this becomes

$$\sum_i h_i W_i = W_A \left[\int_{T_o}^{T} \left(c_{p_A} - c_{p_M} \right) dT + \Delta h^o \right] \tag{9a}$$

where $\Delta h^o = h_A^o - h_M^o$ and is the heat of dissociation of oxygen. The last term of equation (8) becomes, with the aid of equations (6),

$$\begin{aligned} \sum_i \rho D \left(\frac{\partial X_i}{\partial y}\right)\left(\frac{\partial h_i}{\partial y}\right) &= \rho D \left(\frac{\partial T}{\partial y}\right) \sum_i c_{p_i} \left(\frac{\partial X_i}{\partial y}\right) \\ &= \rho D \left(\frac{\partial T}{\partial y}\right)\left(c_{p_A} - c_{p_M}\right)\left(\frac{\partial X_A}{\partial y}\right) \end{aligned} \tag{9b}$$

In the usual temperatures considered for the oxygen dissociation and recombination, $|c_{p_A} - c_{p_M}|$ is very small. Equations (9a) and (9b) are combined and the last two terms of equation (8) are approximately expressed here as

$$\sum_i \left[h_i W_i - \rho D \left(\frac{\partial X_i}{\partial y}\right)\left(\frac{\partial h_i}{\partial y}\right) \right] \approx W_A \Delta h^o$$

Now equation (8) becomes

$$\rho c_p \left(\frac{\partial T}{\partial t} + u \frac{\partial T}{\partial x} + v \frac{\partial T}{\partial y} \right) = \frac{\partial}{\partial y} \left(\lambda \frac{\partial T}{\partial y} \right) + \mu \left(\frac{\partial u}{\partial y} \right)^2 - W_A \Delta h^o \tag{10}$$

This form of the energy equation is used in the subsequent work instead of the original equation (3).

2H

CHEMICAL REACTION KINETICS

There are two classes of reaction kinetics involved in the present work. One is the reaction that takes place in the gas phase (homogeneous reaction), and the other is that which takes place between the gas and the solid at the gas-solid interface (heterogeneous reaction). The heterogeneous reaction pertinent to the present analysis is the surface recombination of oxygen atoms in which the solid acts as a catalyst only.

Homogeneous Chemical Reaction

A 3 3 6

General theory.- Much study has been done on the chemical reactions of oxygen dissociation and recombination. Some of the comprehensive analyses on the subject may be found, for instance, in references 2, 3, and 4.

In the present section, only that portion of the reaction law directly pertinent to the subsequent analysis is explained briefly.

Consider the dissociation and the recombination process of oxygen in air. It is known that the reaction is carried out in the following manner.

$$O_2 + P \underset{k_R}{\overset{k_D}{\rightleftarrows}} 2O + P \tag{11}$$

In the above equation P represents the number of the particles per unit volume which activate the oxygen reaction. It can be O_2 molecules, O atoms, or any other particles in the air. The following relationship is derived by the law of mass action[1] for the reaction represented by the equation (11)

$$N_A = k_R P \left(O_2 K_e - O^2 \right) \tag{12}$$

The equilibrium constant K_e is related to the equilibrium value of m_A by the following equation. (See ref. 2 for more detailed analysis of this section.)

$$K_e(T) = 2C\rho \frac{m_{A,e}^2}{1-m_{A,e}} \tag{13}$$

[1]See reference 4 for the analysis on the law of mass action.

Now, noting that $\rho C = O + 2O_2$ and $m_A = O/(O + 2O_2)$, the expression for the net mass production rate of atoms obtained by combining equations (12) and (13) is

$$W_A = \frac{n\rho C}{\tau}\left(m_{A,e} - m_A\right) \tag{14}$$

where

$$\frac{1}{\tau} = k_R(T)C\rho P\left(\frac{m_{A,e}}{1-m_{A,e}} + m_A\right) \tag{15}$$

A 3 3 6

In the above analysis τ is defined as the relaxation time.

In order for equations (14) and (15) to be of any quantitative value, the values of $k_R(T)$ must be known. Authoritative and accurate experimental values of $k_R(T)$ are yet to be found. The three major theories, one based on collision theory, a second by Eyring, and a third by Wigner predict k_R as the function of $T^{1/2}$, $T^{5/2}$, and $T^{-1/2}$, respectively. Reference 2 analyzes these three theories in detail. The author of the reference felt that the Wigner theory is the most accurate one of the three, and used the following equation in the numerical work.

$$k_R(T) = \frac{50}{\sqrt{T}} \times 10^{-32}\left(\frac{\text{molecules}}{\text{cm}^3}\right)^{-2}\text{sec}^{-1} \tag{16}$$

The specific recombination rate constant was varied with $T^{-3/2}$ in the well-known work of reference 5 and it was different from any of those predicted by the three preceding theories.

Some relatively consistent experimental data of $k_R(T)$ have been reported recently in references 6 and 7. These results show the recombination constant to vary with T^{-2} and their magnitudes fall somewhere between those predicted by the Wigner theory and by reference 5 for temperature range of 2500° to 6000° K.

Linear approximation of the reaction rate law.- The expression for W_A such as given by equation (14) must be first incorporated into the proper conservation equations in order to solve the proposed problem of heat transfer across the nonequilibrium boundary layer. The simultaneous solution of the conservation equations (1), (2), (4), and (10) could then yield the desired result. The conventional technique of the similarity transformation fails to transform the conservation equations to a set of

ordinary differential equations. There is one exception to this statement. The similarity transformation does work at the stagnation point of a blunt object and the problem of heat transfer has been solved for this region in reference 5. The difficulties involved in the similarity transformation were analyzed in some detail in references 5 and 8.

In the absence of the similarity transformation, some sort of perturbation type solution was suggested by several authors including those of references 8 and 9.

A linearization of the reaction rate law is required for the particular perturbation method used in the present work.

A
3
3
6

The linear approximation is based on the following reasoning:

Consider the rate law of equation (14)

$$W_A = \frac{n\rho C}{\tau}\left(m_{A,e} - m_A\right) \qquad (14)$$

Here $m_{A,e}$ represents the equilibrium value of m_A and it is a unique function of the temperature for a given pressure.

The equilibrium constant K_e is calculated by the equilibrium criteria and the method of the calculation can be found in most of the standard books on thermodynamics. Once K_e is found, equation (13) yields the relationship between the equilibrium mass fraction of atoms, the temperature, and the pressure. Sketch (a) represents this

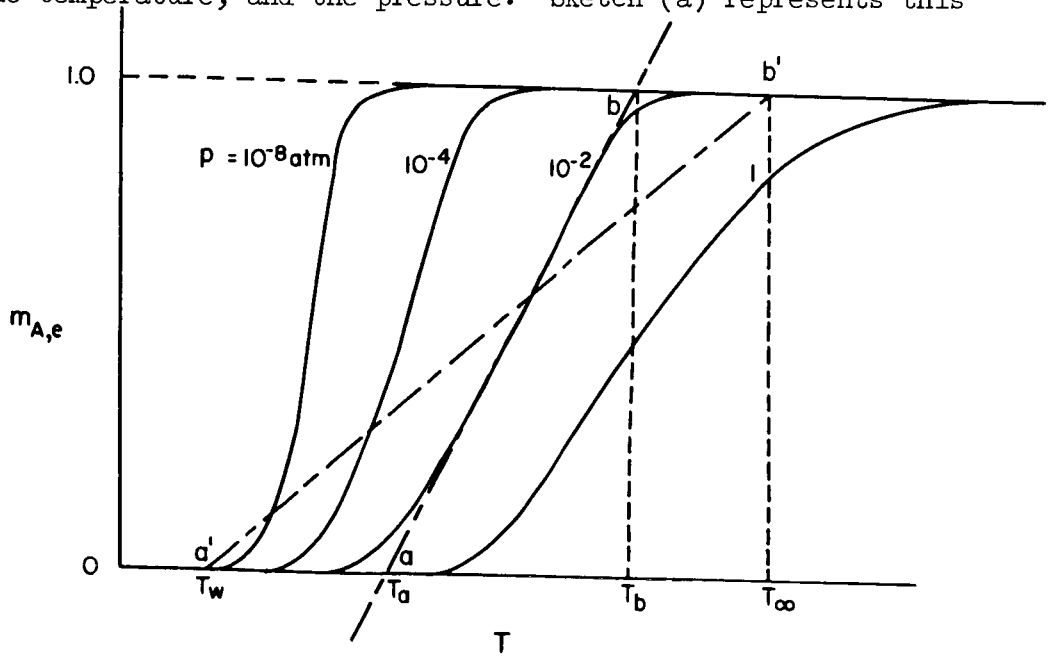

Sketch (a)

relationship for oxygen (see ref. 10). Here the equilibrium curve is first approximated by a straight line. The variable $m_{A,e}$ in equation (14) then can be expressed as a suitable linear function of the temperature.

There are many straight line approximations one can make. A line such as a-b in the sketch approximates an equilibrium line very closely for a given pressure. Such a line, however, does not make any sense for $T_b \leqq T \leqq T_\infty$ and $T_w \leqq T \leqq T_a$ where T_∞ and T_w represent the temperatures at the outer edge of the boundary layer and at the surface respectively.

In the present work, a straight line is chosen to satisfy the following two over-all conditions for the boundary layer:

1. The surface temperature of a vehicle is usually sufficiently low so that the equilibrium mass fraction of atoms corresponding to the wall temperature is zero.

2. The air is assumed to be in equilibrium at the outer edge of the boundary layer.

A straight line satisfying these conditions is shown as a'-b' in sketch (a).

According to the estimate which will be given later, the pressure at the flat afterbody of a hypersonic vehicle is between 10^{-3} and 10^{-1} atmosphere. For such conditions, it is seen from sketch (a) that a line such as a'-b' which connects the values of T_w and T_∞ usually encountered in hypersonic flight approximates the equilibrium lines at least in the average.

Write equation (14) in the following form

$$W_A = \frac{n\rho C}{\tau} m_{A,\infty}(m_e - m) \tag{17}$$

where

$$m = \frac{m_A}{m_{A,\infty}}$$

and

$$m_e = \frac{m_{A,e}}{m_{A,\infty}}$$

Also define a dimensionless temperature

$$\theta = \frac{T - T_w}{T_\infty - T_w}$$

Then the reaction rate law with a linear equilibrium line in relation to the two conditions stated previously is given by

$$W_A = \frac{n\rho C}{\tau} m_{A,\infty}(\theta - m) \tag{18}$$

A
3
3
6

In the study of the one-dimensional, nonequilibrium flow given in reference 2, the relaxation time was first calculated from equation (15) for either the known frozen or the known equilibrium variation of temperature and atom mass fraction along a streamline. The appropriate conservation equations were then solved in connection with the reaction rate equation (14). The results of the solution for the temperature and mass fractions were substituted into equation (15), and the new values were obtained for the relaxation time. The solution of the conservation equations was repeated then with the new relaxation time. Reference 2 showed that this iteration procedure converged very rapidly in most of the cases of one-dimensional flow.

Now consider that in principle the preceding method of solution is to be applied to the present work of Couette flow and boundary-layer problems. The reaction rate law given by equation (18) is then linear since the relaxation time will be expressed in terms of the independent variables from the preceding iteration in each case.

A very similar linear form of the reaction rate law was derived in somewhat different manner and was used in the work of reference 9. A brief summary of the derivation is as follows.

The function $W_A(T,m_A)$ for a given pressure is seen from the physical condition to be continuous and to have at least continuous first-order derivatives. Therefore, W_A can be expanded into a Taylor series about a point on the equilibrium line. When only the first-order terms of the series are considered, W_A becomes

$$W_A = a_o + a_1 m_A + a_2 T$$

where a's are constants.

The dimensionless form of the above equation satisfying the two conditions for the present study stated previously is

$$W_A = \text{constant } m_{A,\infty}(\theta - m) \tag{19}$$

The comparison of equations (18) and (19) shows that the former is in the same form as the latter one when the relaxation time in equation (18) is assumed to be constant throughout.

Finally, consider the relaxation time which is given by equation (15). The symbol τ depends mainly on the specific recombination rate k_R which was analyzed in some detail in the preceding section. It was pointed out there that the mode of the variation of k_R with respect to temperature was rather uncertain as of now. It is stated, also, in reference 2 that the variation of τ in many cases is secondary to that of the rest of the terms in the reaction rate law. Under such circumstances, the relaxation time was assumed to be constant at an average temperature of the flow field and is calculated from equation (15) for various flight conditions in the subsequent analysis.

A 3 3 6

Heterogeneous Chemical Reaction

Some of the comprehensive analysis on the subject of heterogeneous chemical reactions can be found in references 3, 11, 12, and 13.

The portions of the references which are most pertinent to the present work are explained here briefly.

The surface catalytic recombination rate is proportional to jth power of mass concentration of the radicals at the surface. Therefore, the recombination rate $W_{A,w}$ is expressed as

$$W_{A,w} = k_w(\rho_w X_{A,w})^j \tag{20}$$

In the equation, k_w is defined as the specific catalytic recombination rate constant. The exponent, j, shows the order of the reaction. In general, the catalytic recombination process of the dissociated gas, such as oxygen, is known to be a first-order process. For such a reaction, equation (20) becomes simply

$$W_{A,w} = (k_w\rho_w)X_{A,w} \tag{21}$$

where k_w is a property of a particular combination of the reacting gas and the surface whereas ρ_w is the density of the gas at the surface. Many metallic and oxide surfaces have much higher rate constants than nonmetallic ones for a given gas reaction. For instance, at the surface temperature of 700° K, the magnitude of k_w is in the order of 10^{-2} feet per second for glasses whereas it is in the order of 10 feet per second for many metallic surfaces. The product $k_w\rho_w$ usually increases with temperature up to 1300° K or so. For glasses it increases with $T_w^{1/2}$ but for some metals it increases with T_w^7.

COUETTE FLOW SOLUTION

Flow With Finite Homogeneous Reaction Rate

A
3
3
6

The flow characterized by a steady parallel relative motion of two parallel plates containing a viscous fluid is generally known as a Couette flow. In addition to this general concept of the flow, consider that a fluid is being injected uniformly into the stream from the stationary plate. The other plate then must be a porous one so that mass and momentum as well as heat may pass readily through it to keep the entire system in a steady state (see sketch (b)). Such a modified form of the conventional Couette flow model has already been used in the study of mass transfer in reference 14, and in the study of ablation and combustion in reference 15. Consider, also, that the fluid is a nonequilibrium mixture of atoms and molecules, and the chemical reactions of dissociation and recombination are being carried out at a finite rate between the atomic and molecular oxygen components of the fluid.

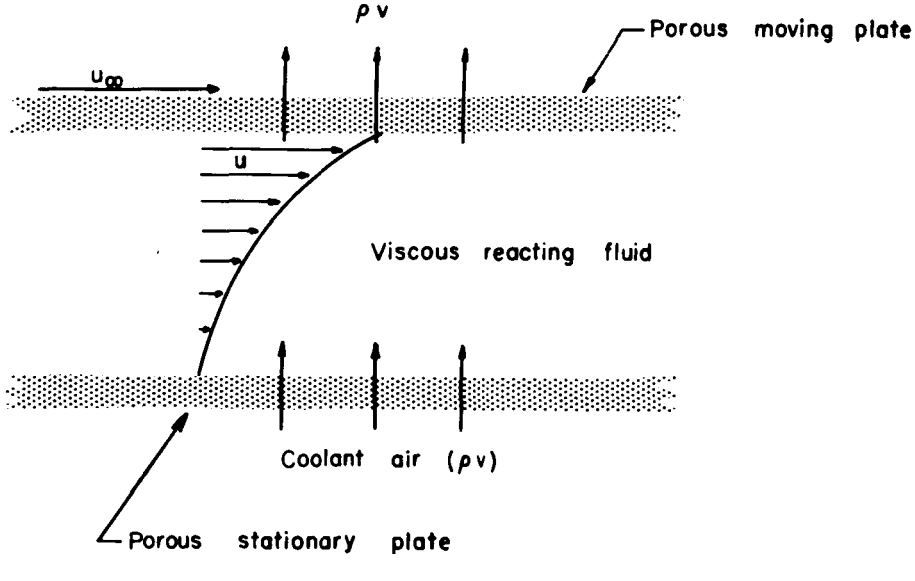

Sketch (b)

The conservation equations (1), (2), (10), and (4) for such a system become, respectively,

$$\frac{d\rho v}{dy} = 0 \tag{22}$$

$$\rho v \frac{du}{dy} = \frac{d}{dy}\left(\mu \frac{du}{dy}\right) \tag{23}$$

$$c_p \rho v \frac{dT}{dy} = \frac{d}{dy}\left(\lambda \frac{dT}{dy}\right) + \mu \left(\frac{du}{dy}\right)^2 - \Delta h^o W_A \tag{24}$$

$$\rho v \frac{dm_A}{dy} = \frac{d}{dy}\left(\rho D \frac{dm_A}{dy}\right) + \frac{W_A}{nC} \tag{25}$$

Here the diffusion equation is written in terms of m_A instead of X_A. This can be done because $m_A = X_A/nC$ and nC is constant as nitrogen in the air is assumed to be chemically inert in the present analysis. As was mentioned previously, the main purpose of the present work is to gain qualitative information on the subject. The numerical work, therefore, should be minimized. For this, the fluid properties, except temperature and composition, are assumed to be constant, and a closed form solution to the Couette flow problem is sought here. The solutions with such assumption would still yield much qualitative information as was the case with the work of reference 16.

In analogy to boundary-layer flow, the moving plate is assumed to represent the outer edge of the boundary layer and the following dimensionless variables are introduced here.

$$U = \frac{u}{u_\infty}, \quad \theta = \frac{T - T_w}{T_\infty - T_w}, \quad m = \frac{m_A}{m_{A,\infty}}, \quad Y = \frac{y}{L}$$

The conservation equations (22) through (25) become by the aid of equation (18)

$$\rho v = \text{constant} \tag{26}$$

$$U'' - \delta U' = 0 \tag{27}$$

$$\theta'' - \delta \mathrm{Pr}\theta' = - \mathrm{PrE}(U')^2 + \frac{1}{\tau_2}(\theta - m) \tag{28}$$

$$m'' - \delta \mathrm{Sc}m' = - \frac{1}{\tau_1}(\theta - m) \tag{29}$$

where

$$\delta = \frac{\rho v L}{\mu}$$

$$\frac{1}{\tau_1} = \frac{L^2}{D}\left(\frac{1}{\tau}\right)$$

$$\frac{1}{\tau_2} = \frac{L^2 \Delta h^{\circ} X_{A,\infty}}{\lambda(T_\infty - T_w)}\left(\frac{\rho}{\tau}\right)$$

A
3
3
6

It is seen that $1/\tau_1$ represents the ratio of diffusion time to the relaxation time.

The conservation equations (27), (28), and (29) are all linear and a unique closed form solution can be obtained for given boundary conditions.

The boundary conditions applied here are based on the following physical conditions.

1. The air at the moving plate is in equilibrium at the plate temperature which is sufficiently high to produce a large amount of dissociation.

2. The stationary plate has either a zero, a finite, or extremely high catalytic rate constant for atom recombination, and its temperature is sufficiently low that the equilibrium mass concentration of oxygen atoms is zero.

3. Air is injected into the stream uniformly from the stationary plate, and the injection rate is given by ρv.

The boundary conditions corresponding to the above-stated physical conditions are as follows:

at Y = 0 (stationary plate)

$$U_w = 0 \tag{30}$$

$$\theta_w = 0 \tag{31}$$

$$m_w' = Sc(\gamma_w + \delta)m_w \quad \text{as} \quad k_w \quad \text{is finite} \tag{32a}$$

$$m_w = 0 \quad \text{as} \quad k_w \quad \text{is extremely high} \tag{32b}$$

A 3 3 6

where

$$\gamma_w = \frac{L\rho k_w}{\mu}$$

at Y = 1 (moving plate)

$$U_\infty = 1 \tag{33}$$

$$\theta_\infty = 1 \tag{34}$$

$$m_\infty = 1 \tag{35}$$

The boundary condition of (32a) is derived by making the following relationship of mass balance for atoms dimensionless at the stationary plate.

$$\rho D \left(\frac{dX_A}{dy}\right)_w - \rho v X_{A,w} = \rho k_w X_{A,w}$$

or

$$\rho D \left(\frac{dm}{dy}\right)_w - \rho v m_w = \rho k_w m_w$$

The left side of the equations represents the net rate of atoms arriving at the stationary plate whereas the right side represents the net rate of disappearance of the atoms by the catalytic reaction and is given by equation (21).

When k_w, and therefore γ_w, becomes extremely large, m_w in equation (32a) must go to 0 since m_w' is finite. Equation (32b) is therefore valid when the recombination occurs extremely fast at the surface. When the stationary plate is totally noncatalytic, the relationship (32a) is valid with $\gamma_w = 0$ in the equation.

The solutions of equations (27), (28), and (29) satisfying the boundary conditions (30) through (35) are obtained as follows:

A
3
3
6

$$U(Y) = \frac{e^{\delta Y} - 1}{e^{\delta} - 1} \tag{36}$$

$$\theta(Y) = C_1 + C_2 B_2 e^{D_2 Y} + C_3 B_3 e^{D_3 Y} + C_4 B_4 e^{D_4 Y} + B_5 e^{2\delta Y} \tag{37}$$

$$m(Y) = C_1 + C_2 e^{D_2 Y} + C_3 e^{D_3 Y} + C_4 e^{D_4 Y} + A_5 e^{2\delta Y} \tag{38}$$

The parameters in the solutions (36) through (38) are given in appendix A.

The total heat transfer to the stationary plate is obtained as follows:

For a finite γ_w

$$q = \lambda \left(\frac{dT}{dy}\right)_w + \Delta h^{\circ} k_w \rho X_{A,w} \tag{39}$$

Making the above equation dimensionless yields

$$Nu_L = \frac{qL}{\lambda(T_\infty - T_w)} = \theta_w' + \frac{X_{A,\infty}\Delta h^{\circ}}{c_p(T_\infty - T_w)} Pr \gamma_w m_w \tag{40}$$

For an extreme γ_w

$$q = \lambda \left(\frac{dT}{dy}\right)_w + \Delta h^\circ \rho D \left(\frac{dX_A}{dy}\right)_w \tag{41}$$

Making the equation dimensionless yields

$$Nu_L = \theta'_w + \frac{X_{A,\infty}\Delta h^\circ}{c_p(T_\infty - T_w)} Lem'_w \tag{42}$$

A 3 3 6

Flow With Frozen Homogeneous Reaction

There are two limiting cases to the problem. They are the cases with the frozen and the equilibrium homogeneous reactions, respectively. The equations and the solutions become much simpler for these cases.

Consider first that the gas-phase reaction is frozen. This is the limit approached as the relaxation time becomes infinitely long compared to the diffusion time. Equations (27), (28), and (29) become

$$U'' - \delta U' = 0 \tag{27}$$

$$\theta'' - \delta Pr\theta' = - PrE(U')^2 \tag{43}$$

$$m'' - \delta Scm' = 0 \tag{44}$$

The solution of these equations is of course very simple and the application of the boundary conditions (30) through (35) to the general solution yields

$$\theta(Y) = \left[1 + \frac{PrE\left(\frac{\delta}{e^\delta - 1}\right)^2 (1 - e^{2\delta})}{2\delta^2(Pr - 2)}\right] \frac{e^{\delta PrY} - 1}{e^{\delta Pr} - 1} + \frac{PrE\left(\frac{\delta}{e^\delta - 1}\right)^2}{2\delta^2(Pr - 2)} (e^{2\delta Y} - 1) \tag{45}$$

$$m(Y) = \frac{B_6 e^{\delta ScY} + \delta Sc - B_6}{\delta Sc - B_6 + B_6 e^{\delta Sc}} \quad \text{for a finite} \quad \gamma_w \tag{46a}$$

$$m(Y) = \frac{e^{\delta ScY} - 1}{e^{\delta Sc} - 1} \quad \text{for an extreme} \quad \gamma_w \tag{46b}$$

The values θ_w, m_w, θ'_w, and m'_w can be obtained directly from the above equations, and substitution of these values into the appropriate equations (40) and (42) yields the desired quantity Nu_L for the case of frozen flow.

Flow With Equilibrium Homogeneous Reaction

Next, consider that the gas is locally in equilibrium at the prevailing condition of the locality. This implies the following facts.

1. The relaxation time is very short compared to the time required for diffusion and convection of the atoms. The reaction rate at a locality, therefore, is controlled completely by the rates of diffusion and convection of the atoms to and from the locality.

2. The relationship between the temperature and the mass fraction of atoms at each point in the fluid satisfies the equilibrium criteria.

In accordance with the above condition 1, an expression is obtained for $(1/\tau_2)(\theta - m)$ in terms of m' and m'' from the diffusion equation (29), and it is substituted into equation (28). Next, in accordance with condition 2, m' and m'' in the resulting equation are set equal to θ' and θ'', respectively, since $m(Y) = \theta(Y)$ when the gas is in equilibrium. There then results:

$$\theta'' - \delta Pr_e \theta' = - \frac{PrE \left(\frac{\delta}{e^{\delta} - 1} \right)^2}{1 + Le \frac{\Delta h^{\circ} X_{A,\infty}}{c_p (T_\infty - T_w)}} e^{2\delta Y} \tag{47a}$$

where

$$Pr_e = \frac{1 + \frac{\Delta h^{\circ} X_{A,\infty}}{c_p (T_\infty - T_w)} \left(\frac{dm}{d\theta} \right)_e}{1 + Le \frac{\Delta h^{\circ} X_{A,\infty}}{c_p (T_\infty - T_w)} \left(\frac{dm}{d\theta} \right)_e} Pr \tag{47b}$$

The particular form of the effective Prandtl number shown above was first derived and was discussed in reference 9.

It is seen that $Pr_e = Pr$ when $Le = 1$.

The solution of equation (47a) is again very simple, and is

$$\theta(Y) = \frac{B_9(e^{2\delta}-1) - 1}{1 - e^{\delta Pr_e}} (e^{\delta Pr_e Y} - 1) + B_7(e^{2\delta Y} - 1) \qquad (48)$$

where

$$B_7 = - \frac{PrE \left(\frac{\delta}{e^{\delta}-1}\right)^2}{2\delta^2 \left[1 + Le \frac{\Delta h^{\circ} X_{A,\infty}}{c_p(T_\infty - T_w)}\right] (2 - Pr_e)}$$

The heat transfer to the stationary wall for this case is independent of the surface catalytic conditions and is given by:

$$Nu_L = \left[1 + Le \frac{\Delta h^{\circ} X_{A,\infty}}{c_p(T_\infty - T_w)}\right] \theta'_w \qquad (49)$$

It is seen from the particular linear reaction rate law used here that $\theta(Y) = m(Y)$ when the fluid is in equilibrium.

STEADY BOUNDARY-LAYER SOLUTION BY RAYLEIGH'S ANALOGY

General Solution

It is known that the steady boundary-layer solution for a solid surface can be approximated by solving for the transient boundary layer on the surface starting impulsively. Such an approximation is called Rayleigh's analogy.

The analogy was somewhat modified in reference 17 to include the effect of mass injection at the surface.

In the present work, the principle of Rayleigh's analogy is extended to include the effect of energy transfer and chemical reaction as well as that of mass transfer.

The major simplification is achieved in Rayleigh's approximation by using the terms with $\partial/\partial t$ which is linear instead of the term with $u(\partial/\partial x)$, which is nonlinear, in the original momentum equation.

The specific problem solved here follows: Consider a porous flat plate which is infinite in size, and is in contact with the fluid above it.

Initially, the temperature of the fluid and the plate is at uniform value of T_∞, and the mass fraction of atoms in the fluid is at the equilibrium value of $X_{A,\infty}$.

A 3 3 6

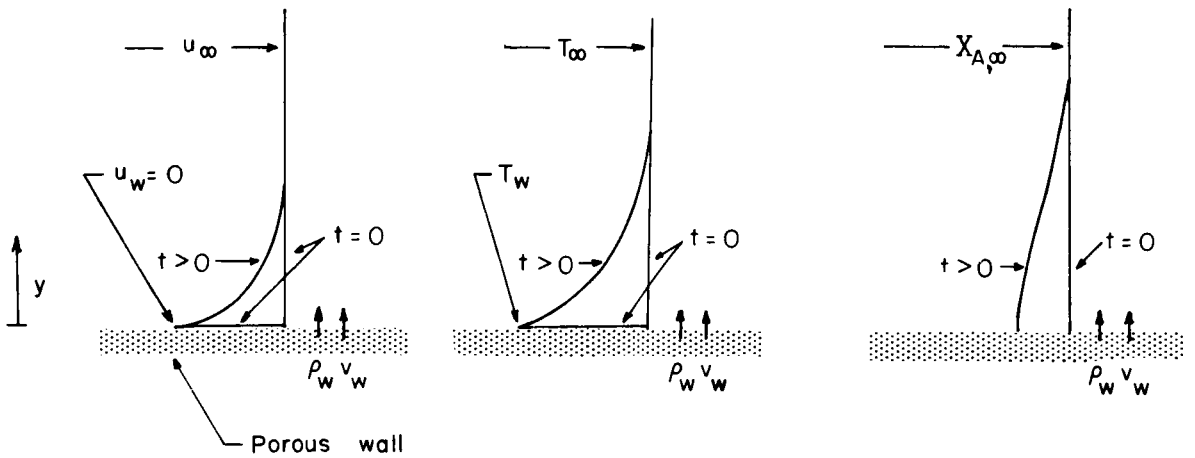

Sketch (c)

Now consider that the following conditions are imposed on the plate suddenly at zero time. (Sketch (c) illustrates the problem.)

1. The plate is started toward the left at uniform velocity of $-u_\infty$. This is the same as the fluid moving toward the right with u_∞.

2. Temperature of the plate is lowered to T_w.

3. Fluid injection is started uniformly over the whole plate and is decreased in accordance with the relationship $v = v_o/\sqrt{t}$ thereafter. Here v_o is a constant.

After the completion of the transient solution, the analogous steady boundary-layer solution is found by setting

$$t = \frac{x}{u_\infty} \tag{50}$$

The pertinent conservation equations are obtained from equations (1), (2), (4), and (10) for the constant fluid properties as follows:

$$\frac{\partial(\rho v)}{\partial y} = 0 \tag{51}$$

$$\frac{\partial u}{\partial t} + v \frac{\partial u}{\partial y} = \nu \frac{\partial^2 u}{\partial y^2} \tag{52}$$

$$\rho c_p\left(\frac{\partial T}{\partial t} + v \frac{\partial T}{\partial y}\right) = \lambda\left(\frac{\partial^2 T}{\partial y^2}\right) + \mu\left(\frac{\partial u}{\partial y}\right)^2 - \Delta h^o W_A \tag{53}$$

$$\rho\left(\frac{\partial m_A}{\partial t} + v \frac{\partial m_A}{\partial y}\right) = \rho D \frac{\partial^2 m_A}{\partial y^2} + \frac{1}{nC} W_A \tag{54}$$

The following dimensionless independent variables are introduced here.

$$\xi = \frac{t}{\tau} \tag{55}$$

$$\eta = \frac{1}{\sqrt{\nu}}\left(\frac{y}{2\sqrt{t}} - v_o\right) \tag{56}$$

The dependent variables are made dimensionless as in the Couette flow case as

$$U = \frac{u}{u_\infty}, \qquad \theta = \frac{T - T_w}{T_\infty - T_w}, \qquad m = \frac{m_A}{m_{A,\infty}}$$

Now the conservation equations are transformed to the subsequent set of dimensionless equations by the use of the new dimensionless dependent variables, and by changing the independent variables t and y to the new ones ξ and η. The expression for W_A is obtained from the linear reaction rate law of equation (18).

$$\frac{1}{4} U'' + \frac{\eta}{2} U' = 0 \tag{57}$$

$$\left(\frac{1}{4Pr}\right)\frac{\partial^2\theta}{\partial\eta^2} + \frac{\eta}{2}\frac{\partial\theta}{\partial\eta} + \frac{1}{4}E(U')^2 = \xi\left[\frac{\partial\theta}{\partial\xi} + \frac{X_{A,\infty}\Delta h^o}{c_p(T_\infty - T_w)}(\theta - m)\right] \tag{58}$$

$$\left(\frac{1}{4Sc}\right)\frac{\partial^2 m}{\partial\eta^2} + \frac{\eta}{2}\frac{\partial m}{\partial\eta} = \xi\left[\frac{\partial m}{\partial\xi} - (\theta - m)\right] \tag{59}$$

The analysis of the nonequilibrium boundary layer is much more complicated than that of the Couette flow and involves a substantial amount of numerical work. Here, therefore, only two extreme surface conditions are considered in order not to complicate further the analysis of the nonequilibrium boundary layer. The two surface conditions are the noncatalytic and the extremely catalytic ones. The method of treatment of the finite catalytic efficiencies in connection with a frozen boundary layer is found in references 11 and 13. It is seen that the treatment given in the references can be incorporated into the present work of nonequilibrium boundary layer, but with much added complexity.

The physical conditions stated at the beginning of this section imply the following boundary conditions for the present problem.

At $\eta = -\frac{v_o}{\sqrt{\nu}}$, $\quad (y = 0)$

$$U_w = 0 \tag{60a}$$

$$v_w = \frac{v_o}{\sqrt{t}} \tag{60b}$$

$$\theta_w = 0 \tag{61}$$

$$\left(\frac{\partial m}{\partial\eta}\right)_w - 2Sc\left(\frac{v_o}{\sqrt{\nu}}\right)m_w = 0 \quad \text{for} \quad k_w = 0 \tag{62a}$$

$$m_w = 0 \quad \text{for extremely large} \quad k_w \tag{62b}$$

At $\eta = \infty$, $\quad (y = \infty)$

$$U_\infty = 1 \tag{63}$$

$$\theta_\infty = 1 \tag{64}$$

$$m_\infty = 1 \tag{65}$$

The boundary conditions (62a) and (62b) came from the atom mass balance at the wall, as was discussed in the previous section on Couette flow. The injection rate at the surface is given by the dimensionless parameter, $v_o/\sqrt{\nu}$. The quantity $v_o/\sqrt{\nu}$ is equal to $v_w\sqrt{t/\nu}$, and the relationship, $t = x/u_\infty$, leads to the expression

A
3
3
6

$$\frac{v_o}{\sqrt{\nu}} = \frac{v_w}{u_\infty}\sqrt{Re} \tag{66}$$

Thus the dimensionless injection parameter used here is equivalent to the conventional Blasius injection parameter $-f_w$.

The momentum equation (57) is integrated readily to satisfy the boundary conditions as

$$U(\eta) = \frac{\operatorname{erf}(\eta) + \operatorname{erf}\left(\frac{v_o}{\sqrt{\nu}}\right)}{1 + \operatorname{erf}\left(\frac{v_o}{\sqrt{\nu}}\right)} \tag{67}$$

The term in equation (58) which includes $(U')^2$ can be rewritten as a function of η with the aid of the solution (67). The solutions of the remaining equations (58) and (59) are obtained here by the following method of perturbation.

Let

$$\theta(\xi,\eta) = \sum_{n=0}^{\infty} \xi^n \theta_n(\eta) \tag{68}$$

$$m(\xi,\eta) = \sum_{n=0}^{\infty} \xi^n m_n(\eta) \tag{69}$$

In order that the present technique of perturbation be successful, θ_n and m_n must be functions of η only. It will be seen in the following perturbed equations that they are indeed functions of η only.

When the above series are substituted into equations (58) and (59), and the terms with the same powers of ξ are equated, the following set of perturbed equations is derived.

$$\frac{1}{4Pr}\theta_o'' + \frac{\eta}{2}\theta_o' + \frac{E}{\pi\left[1 + \operatorname{erf}\left(\frac{v_o}{\sqrt{\nu}}\right)\right]^2} e^{-2\eta^2} = 0 \tag{70}$$

$$\frac{1}{4Sc} m_o'' + \frac{\eta}{2} m_o' = 0 \tag{71}$$

$$\frac{1}{4Pr}\theta_1'' + \frac{\eta}{2}\theta_1' - \theta_1 = \frac{X_{A,\infty}\Delta h^o}{c_p(T_\infty - T_w)}(\theta_o - m_o) \tag{72}$$

$$\frac{1}{4Sc} m_1'' + \frac{\eta}{2} m_1' - m_1 = -(\theta_o - m_o) \tag{73}$$

$$\frac{1}{4Pr}\theta_2'' + \frac{\eta}{2}\theta_2' - 2\theta_2 = \frac{X_{A,\infty}\Delta h^o}{c_p(T_\infty - T_w)}(\theta_1 - m_1) \tag{74}$$

$$\frac{1}{4Sc} m_2'' + \frac{\eta}{2} m_2' - 2m_2 = -(\theta_1 - m_1) \tag{75}$$

. . . . . .

$$\frac{1}{4Pr}\theta_n'' + \frac{\eta}{2}\theta_n' - n\theta_n = \frac{X_{A,\infty}\Delta h^o}{c_p(T_\infty - T_w)}(\theta_{n-1} - m_{n-1}) \tag{76}$$

$$\frac{1}{4Sc} m_n'' + \frac{\eta}{2} m_n' - nm_n = -(\theta_{n-1} - m_{n-1}) \tag{77}$$

. . . . . .

It is seen that each of the above perturbed equations is linear. The boundary conditions for the perturbed equations must be such that the original functions (68) and (69) for θ and m should satisfy the boundary conditions (60) through (65). Such boundary conditions are as follows:

For the zero-order perturbed equations (70) and (71)

$$\theta_{o,w} = 0 \tag{78}$$

$$m'_{o,w} - 2\left(\frac{v_o}{\sqrt{\nu}}\right) Scm_{o,w} = 0 \quad \text{for} \quad k_w = 0 \tag{79}$$

$$m_{o,w} = 0 \quad \text{for} \quad k_w \text{ extremely large} \tag{80}$$

$$\theta_{o,\infty} = 1 \tag{81}$$

$$m_{o,\infty} = 1 \tag{82}$$

For the nth perturbation excluding $n = 0$

$$\theta_{n,w} = 0 \tag{83}$$

$$m'_{n,w} - 2Sc\left(\frac{v_o}{\sqrt{\nu}}\right) m_{n,w} = 0 \quad \text{for} \quad k_w = 0 \tag{84}$$

$$m_{n,w} = 0 \quad \text{for} \quad k_w \text{ extremely large} \tag{85}$$

$$\theta_{n,\infty} = 0 \tag{86}$$

$$m_{n,\infty} = 0 \tag{87}$$

The following describes, briefly, the main points of the method used in the solution of the equation. The details appear in appendix B.

The zero-order perturbed equations (70) and (71) are first integrated to yield

A 3 3 6

$$\theta_o(\eta) = \frac{\operatorname{erf}(\sqrt{Pr}\eta) + \operatorname{erf}\left(\sqrt{Pr}\,\frac{v_o}{\sqrt{\nu}}\right)}{1 + \operatorname{erf}\left(\sqrt{Pr}\,\frac{v_o}{\sqrt{\nu}}\right)} \left\{1 + \frac{2PrE}{\pi\left[1 + \operatorname{erf}\left(\frac{v_o}{\sqrt{\nu}}\right)\right]^2} \sqrt{\frac{\pi}{2 - Pr}} \left[I_1(\infty) - I_1\left(\frac{v_o}{\sqrt{\nu}}\right)\right]\right\}$$

$$- \left\{\frac{2PrE}{\pi\left[1 + \operatorname{erf}\left(\frac{v_o}{\sqrt{\nu}}\right)\right]^2} \sqrt{\frac{\pi}{2 - Pr}} \left[I_1(\eta) - I_1\left(\frac{v_o}{\sqrt{\nu}}\right)\right]\right\} \tag{88}$$

where

$$I_1(\eta) = \int_o^\eta e^{-Prz^2} \operatorname{erf}(\sqrt{2 - Pr}\, z)dz \tag{89}$$

$$m_o(\eta)_{k_w=o} = \frac{\sqrt{\frac{\pi}{4Sc}}\left[\operatorname{erf}(\sqrt{Sc}\eta) + \operatorname{erf}\left(\sqrt{Sc}\,\frac{v_o}{\sqrt{\nu}}\right)\right] + \frac{1}{2Sc}\left(\frac{\sqrt{\nu}}{v_o}\right) e^{-Sc(v_o/\sqrt{\nu})^2}}{\sqrt{\frac{\pi}{4Sc}}\left[1 + \operatorname{erf}\left(\sqrt{Sc}\,\frac{v_o}{\sqrt{\nu}}\right)\right] + \frac{1}{2Sc}\,\frac{\sqrt{\nu}}{v_o}\, e^{-Sc(v_o/\sqrt{\nu})^2}} \tag{90}$$

$$m_o(\eta)_{k_w \to \infty} = \frac{\operatorname{erf}(\sqrt{Sc}\ \eta) + \operatorname{erf}\left(\sqrt{Sc}\,\frac{v_o}{\sqrt{\nu}}\right)}{1 + \operatorname{erf}\left(\sqrt{Sc}\,\frac{v_o}{\sqrt{\nu}}\right)} \tag{91}$$

Next, the general perturbed equations (76) and (77) for $n \neq 0$ are solved as follows.

Consider the homogeneous parts of equations (76) and (77) which are

$$\frac{1}{4Pr}\,\theta_n'' + \frac{\eta}{2}\,\theta_n' - n\theta_n = 0 \tag{92}$$

$$\frac{1}{4Sc}\,m_n'' + \frac{\eta}{2}\,m_n' - nm_n = 0 \tag{93}$$

In general, there are two independent solutions for each of the above homogeneous equations. Two solutions, one for each of the equations, are obtained here in the polynomial form as

$$H_{\theta,n}(\eta) = 1 + \sum_{k=1}^{n} a_{2k}\eta^{2k} \tag{94}$$

where

$$a_{2k} = \frac{n(n-1)(n-2)\cdots(n-k+1)}{(2k)!\left(\frac{1}{4Pr}\right)^{k}}$$

and

$$H_{m,n}(\eta) = 1 + \sum_{k=1}^{n} b_{2k}\eta^{2k} \tag{95}$$

where

$$b_{2k} = \frac{n(n-1)(n-2)\cdots(n-k+1)}{(2k)!\left(\frac{1}{4Sc}\right)^{k}}$$

The particular solutions $H_{\theta,n}$ and $H_{m,n}$ represent one of the two solutions for equations (92) and (93), respectively.

The analytic solutions (94) and (95) of the homogeneous equations are exploited here, and the appropriate Green's functions are constructed to satisfy the homogeneous boundary conditions (83) through (87). The complete solutions for the perturbed equations (76) and (77) satisfying the proper boundary conditions are then obtained in the following integral forms:

$$\theta_n(\eta) = 4Pr\,\frac{X_{A,\infty}\Delta h^{o}}{c_p(T_\infty - T_w)}\int_{-\frac{v_o}{\sqrt{\nu}}}^{\infty} G_{\theta,n}(\eta,z)[\theta_{n-1}(z) - m_{n-1}(z)]e^{Prz^2}dz \tag{96}$$

$$m_n(\eta) = -\,4Sc\int_{-\frac{v_o}{\sqrt{\nu}}}^{\infty} G_{m,n}(\eta,z)[\theta_{n-1}(z) - m_{n-1}(z)]e^{Scz^2}dz \tag{97}$$

where the G's represent the Green's functions and are given by

$$G_{\theta,n}(\eta,z) = \begin{cases} \dfrac{1}{I_{\theta,n}(\infty) + I_{\theta,n}\left(\dfrac{v_o}{\sqrt{\nu}}\right)} \alpha_{n,w}(\eta)\alpha_{n,\infty}(z) & \text{for } z \geqq \eta \\ \dfrac{1}{I_{\theta,n}(\infty) + I_{\theta,n}\left(\dfrac{v_o}{\sqrt{\nu}}\right)} \alpha_{n,\infty}(\eta)\alpha_{n,w}(z) & \text{for } z \leqq \eta \end{cases} \tag{98}$$

When $k_w = 0$

$$G_{m,n}(\eta,z) = \begin{cases} \dfrac{1}{I_{m,n}(\infty) + I_{m,n}\left(\dfrac{v_o}{\sqrt{\nu}}\right) + C_m} \beta_{n,w}(\eta)\beta_{n,\infty}(z) & \text{for } z \geqq \eta \\ \dfrac{1}{I_{m,n}(\infty) + I_{m,n}\left(\dfrac{v_o}{\sqrt{\nu}}\right) + C_m} \beta_{n,\infty}(\eta)\beta_{n,w}(z) & \text{for } z \leqq \eta \end{cases} \tag{99a}$$

and when $k_w \to \infty$

$$G_{m,n}(\eta,z) = \begin{cases} \dfrac{1}{I_{m,n}(\infty) + I_{m,n}\left(\dfrac{v_o}{\sqrt{\nu}}\right)} \beta_{n,w}(\eta)\beta_{n,\infty}(z) & \text{for } z \geqq \eta \\ \dfrac{1}{I_{m,n}(\infty) + I_{m,n}\left(\dfrac{v_o}{\sqrt{\nu}}\right)} \beta_{n,\infty}(\eta)\beta_{n,w}(z) & \text{for } z \leqq \eta \end{cases} \tag{99b}$$

where

$$\alpha_{n,w}(\eta) = H_{\theta,n}(\eta)\left[I_{\theta,n}(\eta) + I_{\theta,n}\left(\frac{v_o}{\sqrt{\nu}}\right)\right] \tag{100}$$

$$\alpha_{n,\infty}(\eta) = - H_{\theta,n}(\eta)\left[I_{\theta,n}(\infty) - I_{\theta,n}\left(\frac{v_o}{\sqrt{\nu}}\right)\right] \tag{101}$$

$$\beta_{n,w}(\eta) = H_{m,n}(\eta)\left[I_{m,n}(\eta) + I_{m,n}\left(\frac{v_o}{\sqrt{\nu}}\right) + C_m\right] \quad \text{for} \quad k_w = 0 \tag{102a}$$

$$\beta_{n,w}(\eta) = H_{m,n}(\eta)\left[I_{m,n}(\eta) + I_{m,n}\left(\frac{v_o}{\sqrt{\nu}}\right)\right] \quad \text{for} \quad k_w = \infty \tag{102b}$$

$$\beta_{n,\infty}(\eta) = - H_{m,n}(\eta)\left[I_{m,n}(\infty) - I_{m,n}(\eta)\right] \tag{103}$$

$$C_m = \frac{1}{H_{m,n}\left(-\frac{v_o}{\sqrt{\nu}}\right) e^{Sc(v_o/\sqrt{\nu})^2}\left[2Sc\,\frac{v_o}{\sqrt{\nu}}\,H_{m,n}\left(-\frac{v_o}{\sqrt{\nu}}\right) - H'_{m,n}\left(-\frac{v_o}{\sqrt{\nu}}\right)\right]} \tag{104}$$

$$I_{\theta,n}(\eta) = \int_o^\eta \frac{dz}{[H_{\theta,n}(z)]^2 e^{Prz^2}} \tag{105}$$

and

$$I_{m,n}(\eta) = \int_o^\eta \frac{dz}{[H_{m,n}(z)]^2 e^{Scz^2}} \tag{106}$$

The heat transfer to the surface is given by

$$q = \lambda\left(\frac{\partial T}{\partial y}\right)_w \quad \text{for} \quad k_w = 0 \tag{107}$$

and

$$q = \lambda\left(\frac{\partial T}{\partial y}\right)_w + \Delta h^o \rho D\left(\frac{\partial X_A}{\partial y}\right)_w \quad \text{for} \quad k_w \text{ extremely large} \tag{108}$$

Making the above equations dimensionless yields, respectively,

$$\frac{Nu}{\sqrt{Re}} = \frac{1}{2}\left(\frac{\partial\theta}{\partial\eta}\right)_w \qquad \text{for} \quad k_w = 0 \tag{109}$$

and

$$\frac{Nu}{\sqrt{Re}} = \frac{1}{2}\left[\left(\frac{\partial\theta}{\partial\eta}\right)_w + Le\,\frac{X_{A,\infty}\Delta h^o}{c_p(T_\infty - T_w)}\left(\frac{\partial m}{\partial\eta}\right)_w\right] \qquad \text{for} \quad k_w \quad \text{extremely large} \tag{110}$$

In the derivation of the relationships (109) and (110), the analogy to the steady boundary layer was made by setting $t = x/u_\infty$ and the Nusselt number was defined as $qx/\lambda(T_\infty - T_w)$. The values of $(\partial\theta/\partial\eta)_w$ and $(\partial m/\partial\eta)_w$ necessary in the evaluation of $Nu/\sqrt{Re}$ are obtained from the series (68) and (69) as

$$\left(\frac{\partial\theta}{\partial\eta}\right)_w = \sum_{n=o}^{\infty} \xi^n \theta_n' \left(-\frac{v_o}{\sqrt{\nu}}\right) \tag{111}$$

and

$$\left(\frac{\partial m}{\partial\eta}\right)_w = \sum_{n=o}^{\infty} \xi^n m_n' \left(-\frac{v_o}{\sqrt{\nu}}\right) \tag{112}$$

Range of Solutions Obtainable

It is obvious from the series representations of the solutions given by equations (68), (69), (111), and (112) that the range of ξ for which the solutions can be obtained by the method of perturbation is quite limited. The exact range of ξ for convergence of the series is not known. It is seen, however, that ξ can not be much above 1. The symbol ξ was defined as t/τ and it is the ratio of the flow characteristic time to the relaxation time. The boundary layer is practically frozen when $\xi << 1$, and it is in equilibrium when $\xi >> 1$. When $\xi \approx 1$, the boundary layer is definitely in nonequilibrium and the finite reaction rate must be considered. The main purpose of the present qualitative study is accomplished if the solution can be obtained for $\xi \approx 1$.

It is worthwhile at this point to discuss the actual range of t/τ which may be encountered by a boundary layer of the sort considered here. The pressure at the stagnation point of a blunt body traveling at hypersonic speed in the range of 100,000- to 200,000-feet altitude is found to vary approximately between 10^{-2} and 1 atmosphere according to reference 18. At the region of a vehicle considered here where the pressure gradient is negligible, the pressure is very much less than that at the stagnation point. If it is assumed that the pressure in the boundary layer considered is less than that at the stagnation point by an order of magnitude, it would be between 10^{-3} and 10^{-1} atmosphere.

Figure 1, which is obtained directly from figure 8 of reference 2, shows the variation of the product τp with respect to the temperature. The relaxation times were calculated with the aid of Wigner theory (eq. (16)). The surface temperature of a vehicle is usually less than $1{,}000^{\circ}$ K. Then for an assumed average temperature of $3{,}000^{\circ}$ K for the boundary layer, the relaxation time can be approximately estimated to be between 10^{-3} and 1 second for the pressure range of 10^{-3} to 10^{-1} atmosphere.

A 3 3 6

Now consider the ratio $t/\tau = x/\tau u_{\infty}$. The distance of interest along the plate is usually not more than 10 feet. The magnitude of u_{∞} is in the order of 10^4 feet per second. Then for these values, the range of ξ becomes between 10^{-3} and 1. Therefore, the solutions of most interest here seem to be those for $\xi \leqq 1$, and these solutions can be obtained by the perturbation technique.

Frozen Boundary Layer

The boundary layer becomes chemically frozen as the relaxation time becomes infinitely large in comparison to the flow characteristic time. The ratio ξ then approaches 0, and the energy and diffusion equations (58) and (59) become identical to the zeroth perturbed equations (70) and (71), respectively. Therefore, the solutions given by equations (88) through (91) represent the solutions for the frozen case.

Equilibrium Boundary Layer

The physical implications concerning the gas in a local equilibrium were discussed in the section on Couette flow.

The following equation is derived by combining the two conservation equations (58) and (59)

$$\frac{1}{4Pr_e}\theta'' + \frac{\eta}{2}\theta' + \frac{E}{\pi\left[1 + \frac{X_{A,\infty}\Delta h^o}{c_p(T_\infty - T_w)}\right]\left[1 + \operatorname{erf}\left(\frac{v_o}{\sqrt{\nu}}\right)\right]^2} e^{-2\eta^2} = 0 \qquad (113)$$

This equation is in the same form as equation (70) whose solution is equation (88). Remembering that $\theta(\eta) = m(\eta)$ when the fluid is in equilibrium, the $\theta(\eta)$ and $m(\eta)$ profiles can be obtained directly from equation (88) by replacing Pr by Pr_e and E by

$$\frac{E}{1 + \frac{X_{A,\infty}\Delta h^o}{c_p(T_\infty - T_w)}}$$

A 3 3 6

The heat transfer to the surface is given by the following expression for all catalytic conditions of the surface

$$\frac{Nu}{\sqrt{Re}} = \frac{1}{2}\left[1 + Le\,\frac{X_{A,\infty}\Delta h^o}{c_p(T_\infty - T_w)}\right]\theta_w' \qquad (114)$$

NUMERICAL RESULTS AND DISCUSSION

Couette Flow

It is seen, from references 3, 5, and 12, that the values of 0.71 and 1.4 are fair estimates for Prandtl and Lewis numbers, respectively, in hypersonic heat-transfer work. These property values are used in the numerical calculations of the present analysis. The values of two additional parameters must be specified before the numerical elaborations can be started. They are the Eckert number and the parameter $X_{A,\infty}\Delta h^o/c_p(T_\infty - T_w)$. The Eckert number is defined as $u_\infty^2/c_p(T_\infty - T_w)$ and it represents the ratio of the heat-transfer potential due to kinetic energy to that due to the sensible thermal energy. The parameter $X_{A,\infty}\Delta h^o/c_p(T_\infty - T_w)$, on the other hand, represents the ratio of the heat-transfer potential due to the chemical energy to that due to the sensible thermal energy. Here, the following values are used which are thought to be reasonable for the air which passed through a shock strong enough to dissociate the oxygen completely.

PrE = 2

$$\frac{X_{A,\infty}\Delta h^{o}}{c_p(T_\infty - T_w)} = 2$$

Figures 2(a) and 2(b) show the typical variations of heat transfer calculated for the two fluid injection rates of $\delta = 0$ and $\delta = 2$, respectively. The expected trend of the increasing heat transfer with homogeneous and heterogeneous specific reaction rates is evident. It is seen in the figures that the heat transfer varies considerably with respect to the specific homogeneous reaction rate, $1/\tau_1$, for the lower catalytic efficiencies of the surface. The maximum variations between the frozen and the equilibrium reactions depend mainly on the parameter $X_{A,\infty}\Delta h^{o}/c_p(T_\infty - T_w)$ for a given fluid injection rate. The larger the parameter the greater is the magnitude of the variation. The sensitivity of the heat transfer with respect to the specific homogeneous reaction rate decreases quite rapidly as the catalytic surface efficiency is increased, and it becomes practically invariant to $1/\tau_1$ at the high catalytic recombination rates.

A 3 3 6

The heat transfer is very sensitive to the catalytic condition of the surface up to very large values of $1/\tau_1$. Heat transfer becomes independent of the surface catalytic condition as the gas approaches locally the equilibrium states.

The relative sensitivity of heat transfer with respect to the specific heterogeneous and homogeneous reaction rates can be seen in the figures. For $\delta = 0$, for instance, it takes approximately a 50-fold increase in the surface catalytic parameter γ_w to raise the Nusselt number from 3 to 4.7; whereas, it takes over a 1000-fold increase in the specific homogeneous reaction rate, $1/\tau_1$, to do the same. Heat transfer, therefore, in general, is much more sensitive to the surface catalytic condition than the gas-phase reaction rate. This is because the reaction which occurs at the surface affects the heat transfer more directly than that which takes place in the gas stream away from the surface.

Figure 3 shows some typical velocity profiles for Couette flows.

The effect of the specific gas-phase reaction rate on the chemical state of the gas itself is seen in figure 4. This figure is for the case of δ and γ_w equal to 0. It is seen that the gas approaches an equilibrium state, as is evidenced by the decreasing values of $|\theta - m|$, as the specific reaction rate is increased.[2] The gas further away from

[2]Note that, from the particular linearized rate law of equation (18) used here for the gas-phase reaction, $\theta(Y) = m(Y)$ is an indication of the equilibrium state in the gas. Also $(\theta - m)$ represents the rate of the nonequilibrium reaction since the relaxation time is assumed to be constant.

the stationary wall reaches the equilibrium state first then the gas near the wall approaches it rather slowly. The nonequilibrium condition of the gas adjacent to the wall persists even for very large values of $1/\tau_1$.

The added effect of finite catalytic surface recombination rates is seen in figure 5. For the near frozen gas-phase reaction, the condition of the gas at the wall is immediately brought closer to the equilibrium state as the heterogeneous chemical reaction is now allowed to proceed at a finite rate at the surface. This also changes the shapes of the θ and m profiles through the gas. The surface catalytic reaction, therefore, affects the homogeneous reaction when the gas-phase reaction is very slow. It is seen, however, that the gas-phase reaction rate comes to depend mostly on its own specific reaction rate, except near the wall, as the specific homogeneous reaction rate increases. A comparison of figures 4 and 5 shows that even for a relatively low homogeneous reaction rate of 30, the region of influence of the catalytic reaction on the gas-phase reaction does not extend beyond $Y \approx 0.4$. At a higher gas-phase specific reaction rate of 200, the region of the influence is limited practically to very adjacent gas layers. It is important, however, to notice that the influence of the surface condition persists near the wall, and it has a nonnegligible effect on the heat transfer even for the relatively high gas-phase reaction rates (see fig. 2).

Figure 6 shows the θ and m profiles for an extremely catalytic wall. The gas at the wall is now in equilibrium because of the infinite rate of reaction. The degree of departure from the equilibrium state for the gas away from the wall is still mainly dependent on the homogeneous specific reaction rate. It is seen that the catalytic surface reaction with such a large value of γ_w, however, has a distinct effect on the entire flow field. The catalytic surface as an infinite sink drains the atoms off the gas stream so fast that the concentration of atoms is below the equilibrium values throughout the gas for all the finite homogeneous reaction rates. The reaction of dissociation, therefore, takes place in the gas as it approaches the equilibrium state instead of the reaction of recombination. This effect on heat transfer is seen in figures 2(a) and 2(b). The dotted lines in the figures represent the conductive part of the total heat transfer which is represented by the solid lines. The differences in the ordinate between the two lines then represent the heat transfer due to the atom recombination at the stationary wall. The heat transfer to the wall is by conduction alone when $\gamma_w = 0$. For $\gamma_w = 5$, the recombination is the predominant reaction in the gas phase so that the conductive part of the heat transfer increases steadily as $1/\tau_1$ is increased. The heat transfer due to the catalytic reaction at the surface is decreased at the same time. Only dissociation, on the other hand, takes place in the gas phase when $\gamma_w = \infty$, producing more atoms as the homogeneous reaction rate is increased. The heat transfer due to the surface recombination is increased and the conductive part is decreased as $1/\tau_1$ becomes greater. Finally, for a sufficiently high but a finite catalytic efficiency of the surface, such as for $\gamma_w = 50$, it is seen

that the conductive part of the heat transfer decreases first and then it increases as the gas-phase reaction is continually increased. This phenomenon comes about as the predominant reaction in the gas phase is shifted from dissociation to recombination. This situation is seen more clearly from figure 7. Here the parameter $(\theta - m)$, which is directly proportional to the local homogeneous reaction rate, is plotted against Y for $\delta = 0$. The chemical reaction in the gas phase is predominantly that of dissociation for $1/\tau_1 = 30$. When $1/\tau_1$ is increased to 200, on the other hand, most of the gas is in equilibrium except near the wall where the process of recombination is taking place. It is seen in figure 2 that these effects of γ_w and $1/\tau_1$ on the θ and m profiles through the gas do not have any pronounced effect on the total heat transfer.

A 3 3 6

The particular relative occurrences of dissociation and recombination in the gas phase and the particular mode of the partition between the two parts of the heat transfer depend largely on the particular boundary conditions and the reaction rate law used.

The added effect of the fluid injection is seen in figures 8 through 12.

Figure 8 shows the variation of heat transfer with respect to the injection parameter δ for six different combinations of $1/\tau_1$ and γ_w. It shows that a substantial decrease in heat transfer is accomplished by fluid injection in all the cases.

It is seen from figures 8(a) and 8(d) that when either of the two reaction rates, homogeneous or heterogeneous, is very slow the increase in the other results in a greater decrease in heat transfer for a given fluid injection rate. The similar conclusion was drawn in reference 19 from the analysis of a frozen boundary layer at the stagnation region of hypersonic vehicles. The reason for this phenomenon can be seen, for example, from the comparisons of figures 4 and 9, and 5 and 10, respectively. The first two figures show the θ and m profiles when the catalytic reaction at the stationary wall is frozen; whereas the last two figures show those when the wall has a finite catalytic efficiency. A comparison of figures 4 and 9 shows that the fluid injection plays a substantial role in bringing the fluid closer to an equilibrium state near the wall especially for the lower values of $1/\tau_1$. The fluid injection, therefore, considerably decreases the recombination process near the wall. Comparison of figures 5 and 10, on the other hand, shows that this role of the fluid injection is not so pronounced as the surface becomes more catalytic since the γ_w of the surface then dominantly influences the region near the wall. The comparisons of the figures also show that the homogeneous reaction away from the wall is not altered to any great degree by the fluid injection. From these analyses, it is seen that, excluding the case for either a near frozen homogeneous or a near frozen heterogeneous reaction, the main effect of fluid injection is to shield the surface from the conduction of sensible heat and from

the diffusion of the atoms to the surface. This phenomenon is seen clearly in figure 11. As the fluid injection is increased, the chemical reactions are not changed appreciably, but the temperature gradient and the mass concentration of atoms at the wall are decreased steadily. One preset condition of the problem must be remembered at this point. The problem is solved and analyzed here assuming that the relaxation time for the gas-phase reaction is uniform throughout the flow field. The relaxation time, in practice, varies with the temperature, and the effect of the fluid injection on the relaxation time via decreased temperature must be incorporated into the problem also.

Boundary-Layer Flow

The property values and the Eckert number used for the numerical examples of the boundary-layer flow are the same as those used for the Couette flow. The parameter $X_{A,\infty}\Delta h^{o}/c_p(T_\infty-T_w)$ is considered to be unity here, and it is different from the value of 2 used for the Couette flow case. This gives a little simplification in the the numerical computations.

It is seen in the preceding analysis of the Couette flow that the heat transfer is independent of the homogeneous reaction when the surface is extremely catalytic. The numerical computations are, therefore, carried out here for the cooled, noncatalytic surface only.

Figure 12 shows some of the typical velocity profiles through the boundary layer.

The main numerical work of the present problem lay in the evaluation of the integrals, I_1, $I_{\theta,n}$, and $I_{m,n}$ for $n \neq 1$,[3] and the integrals for θ_n and m_n. It is seen from the expressions (89), (96), (97), (105), and (106) that all the integrals involved are actually quite straightforward. It is also seen from the analysis that the integrals $I_{\theta,n}$ and $I_{m,n}$ need to be evaluated only once for each n, and the same integrals can be used for all fluid injection rates considered.

The calculation of the perturbations through the fourth or fifth order ones yielded sufficiently accurate values of heat transfer for ξ up to 1.2.

Figure 13 shows the deviations of the heat transfer from the frozen cases for different values of ξ. The deviations are shown as percentages of the maximum heat-transfer variations between the frozen and the equilibrium cases for three different injection rates. It is seen in the figure that the deviation of heat transfer from the respective frozen

[3]The analytic expressions for $I_{\theta,1}$ and $I_{m,1}$ are obtained in appendix B.

case is lessened for a given ξ as the injection rate is increased. This implies that, for a given relaxation time, the effect of the atom recombination on the heat transfer to the surface at a given distance downstream from the leading edge becomes less pronounced as fluid is injected into the boundary layer.

Figures 14, 15, and 16 show the temperature and the atom concentration profiles through the boundary layer for the same three fluid injection rates as before. It is seen in the figures that the atom concentration is decreased near the wall as the fluid is injected and it brings the fluid closer to the equilibrium state there. The recombination rate is therefore decreased considerably near the wall by the injection at least for $\xi \leqq 1.2$. This seems to be the main reason for the decreased effect of a given relaxation time on the heat transfer when fluid is injected.

As ξ is increased much beyond 1.2, it seems reasonable to think, from the analysis on the Couette flow, that the reaction rate will become practically independent of the fluid injection, and it will be predominantly controlled by the relaxation time.

It was estimated in the previous section "Steady Boundary-Layer Solution by Rayleigh's Analogy" that the range of ξ which was of most interest here was between 10^{-3} and 1. Assuming, then, that this estimation is not too far off, figure 13 shows most of the probable range of departures of heat transfer from the frozen case. According to the figure, then, the maximum probable departure in heat transfer is only about 35 percent of the total variation between the frozen and the equilibrium cases. It is also seen, from the general slopes of the deviation curves of figure 13, that it will take unreasonably long distances for the fluid to reach near equilibrium state.

CONCLUDING REMARKS

The simultaneous effect of the finite rate recombination of atoms and the fluid injection on the heat transfer to a flat surface was studied theoretically.

The study was made for a Couette flow and for a steady boundary-layer flow which was approximated by Rayleigh's analogy.

The major approximations involved in the analysis were as follows:

1. All the property values were considered to be constant except the temperature and the composition of the gas.

2. Nitrogen in air was assumed to be chemically inert and only the oxygen dissociation and recombination were considered.

3. Air at the moving plate for Couette flow and at the edge of the boundary layer for Rayleigh's problem was assumed to be in chemical equilibrium.

4. A special linear approximation of the homogeneous reaction rate law was made.

A closed-form solution to the Couette flow and a semiclosed form solution by perturbation technique to the boundary-layer flow were derived with the above-stated approximation.

For the Couette flow, the numerical calculations of heat transfer to the cooled surface with finite catalytic efficiencies were made for different homogeneous reaction and fluid injection rates. In the numerical calculation for the boundary-layer flow, the cooled surface was considered to be noncatalytic throughout.

A
3
3
6

The major results of the analysis are as follows.

Couette Flow

When either one of the two reaction rates, homogeneous or heterogeneous, is extremely high, heat transfer is practically independent of the other reaction rate. On the other hand, when both of the reaction rates are of similar magnitude, it is seen that heat transfer is more sensitive to specific surface reaction rate than the specific gas-phase reaction rate.

The homogeneous and the heterogeneous reaction rates are mainly controlled by the relaxation time and the specific catalytic recombination rate, respectively, and they are practically independent of the fluid injection rate except for the cases of very low specific reaction rates. The major role of fluid injection is therefore to shield the surface from the conduction of sensible heat and from the diffusion of atoms.

Boundary-Layer Flow

For a boundary layer developing from the leading edge of a finite plate, the effect of the gas-phase recombination is to raise the heat transfer to a finite plate about one-third of the way, at the most, toward the equilibrium value from the frozen case. This estimate was based on the condition of air at the edge of the boundary layer approximately corresponding to that at a flat afterbody of a blunt nosed hypersonic vehicle.

The surface catalytic efficiency, on the other hand, may increase considerably toward the leading edge since the surface temperature there tends to be higher in practice and the catalytic recombination can cause the heat transfer to approach that for the equilibrium value.

The injection of fluid into the boundary layer decreases the effect of the gas-phase recombination on the heat transfer for a given relaxation time and position along the surface. It should be remembered here that the relaxation time depends considerably on the temperature in practice.

Finally, all the remarks made here must be interpreted only within the limitations imposed on the entire work by the approximations stated previously.

A
3
3
6

Ames Research Center
National Aeronautics and Space Administration
Moffett Field, Calif., Oct. 20, 1959

APPENDIX A

PARAMETERS FOR COUETTE FLOW SOLUTIONS (36) THROUGH (38)

The D's (D_2, D_3, and D_4) in the solutions are the three unequal and real roots of the algebraic equation

$$D^3 + A_1 D^2 + A_2 D + A_3 = 0$$

A
3
3
6

The other constants are given as follows:

$$A_1 = -\delta Pr\left(\frac{1}{Le} + 1\right)$$

$$A_2 = -\left(\frac{1}{\tau_1} + \frac{1}{\tau_2} - \delta^2 PrSc\right)$$

$$A_3 = \delta Pr\left(\frac{1}{\tau_1} + \frac{1}{\tau_2 Le}\right)$$

$$A_4 = PrE\left(\frac{\delta}{e^{\delta}-1}\right)^2\left(\frac{1}{\tau_1}\right)$$

$$A_5 = \frac{A_4}{2\delta(8\delta^3 + 4A_1\delta^2 + 2A_2\delta + A_3)}$$

$$B_2 = 1 + \delta Sc\tau_1 D_2 - \tau_1 D_2^{\,2}$$

$$B_3 = 1 + \delta Sc\tau_1 D_3 - \tau_1 D_3^{\,2}$$

$$B_4 = 1 + \delta Sc\tau_1 D_4 + \tau_1 D_4^{\,2}$$

$$B_5 = A_5(1 + 2\delta^2 Sc\tau_1 - 4\tau_1\delta^2)$$

$$B_6 = Sc(\gamma_w + \delta)$$

The constants C are obtained from the following sets of four linear algebraic equations shown in the matrix form:

For a finite γ_w

$$\begin{bmatrix} 1 & e^{D_2} & e^{D_3} & e^{D_4} \\ 1 & B_2 & B_3 & B_4 \\ 1 & B_2 e^{D_2} & B_3 e^{D_3} & B_4 e^{D_4} \\ B_6 & B_6 - D_2 & B_6 - D_3 & B_6 - D_4 \end{bmatrix} \begin{bmatrix} C_1 \\ C_2 \\ C_3 \\ C_4 \end{bmatrix} = \begin{bmatrix} 1 - A_5 e^{2\delta} \\ - B_5 \\ 1 - B_5 e^{2\delta} \\ A_5(2\delta - B_6) \end{bmatrix}$$

A 3 3 6

For extremely large γ_w

$$\begin{bmatrix} 1 & 1 & 1 & 1 \\ 1 & B_2 & B_3 & B_4 \\ 1 & e^{D_2} & e^{D_3} & e^{D_4} \\ 1 & B_2 e^{D_2} & B_3 e^{D_3} & B_4 e^{D_4} \end{bmatrix} \begin{bmatrix} C_1 \\ C_2 \\ C_3 \\ C_4 \end{bmatrix} = \begin{bmatrix} - A_5 \\ - B_5 \\ 1 - A_5 e^{2\delta} \\ 1 - B_5 e^{2\delta} \end{bmatrix}$$

APPENDIX B

GENERAL SOLUTION OF THE PERTURBED EQUATIONS

The equations to be solved are:

$$\frac{1}{4Pr}\theta_n'' + \frac{\eta}{2}\theta_n' - n\theta_n = \frac{X_{A,\infty}\Delta h^o}{c_p(T_\infty - T_w)}(\theta_{n-1} - m_{n-1}) \tag{76}$$

$$\frac{1}{4Sc}m_n'' + \frac{\eta}{2}m_n' - nm_n = -(\theta_{n-1} - m_{n-1}) \tag{77}$$

A 3 3 6

with the following boundary conditions:

at $\eta = -\frac{v_o}{\sqrt{\nu}}$, $\quad (y = 0)$

$$\theta_{n,w} = 0 \tag{83}$$

$$m_{n,w}' - 2Sc\left(\frac{v_o}{\sqrt{\nu}}\right)m_{n,w} = 0 \quad \text{for} \quad k_w = 0 \tag{84}$$

$$m_{n,w} = 0 \quad \text{for} \quad k_w \to \infty \tag{85}$$

at $\eta = \infty$, $\quad (y = \infty)$

$$\theta_{n,\infty} = 0 \tag{86}$$

$$m_{n,\infty} = 0 \tag{87}$$

The homogeneous equations are:

$$\frac{1}{4Pr}\theta_n'' + \frac{\eta}{2}\theta_n' - n\theta_n = 0 \tag{92}$$

$$\frac{1}{4Sc} m_n'' + \frac{\eta}{2} m_n' - n m_n = 0 \tag{93}$$

The two solutions, one for each, of the homogeneous equations (92) and (93) are obtained by substituting the following infinite series into the appropriate equations

$$\theta_n(\eta) = 1 + \sum_{k=1}^{\infty} a_k \eta^k$$

$$m_n(\eta) = 1 + \sum_{k=1}^{\infty} b_k \eta^k$$

The solutions of the homogeneous equations are expressed by $H_{\theta,n}(\eta)$ and $H_{m,n}(\eta)$, and are given by the polynomials (94) and (95)

$$H_{\theta,n}(\eta) = 1 + \sum_{k=1}^{n} a_{2k} \eta^{2k} \tag{94}$$

where

$$a_{2k} = \frac{n(n-1)(n-2) \cdots (n-k+1)}{(2k)!\left(\frac{1}{4Pr}\right)^k}$$

$$H_{m,n}(\eta) = 1 + \sum_{k=1}^{n} b_{2k} \eta^{2k} \tag{95}$$

where

$$b_{2k} = \frac{n(n-1)(n-2) \cdots (n-k+1)}{(2k)!\left(\frac{1}{4Sc}\right)^k}$$

Now consider a second-order linear equation, in general, with a set of homogeneous boundary conditions.

$$fR''(r) + f'R'(r) - gR(r) = -\varphi(r) \tag{B1}$$

$$A_1R(a) + A_2R'(a) = 0 \qquad \text{(B2a)}$$

$$A_3R(b) + A_4R'(b) = 0 \qquad \text{(B2b)}$$

In the above equation, R represents a continuous function of the independent variable r, and it has continuous first- and second-order derivatives in the interval (a,b). The functions f, f', and g are also continuous functions of r in the same interval, and f is positive. In the boundary conditions A's are given constants of which A_1 and A_2 are not both 0, and A_3 and A_4 are not both 0. Notice that equation (B1) is written in the self-adjoint form. Let R_a and R_b be two independent solutions of the homogeneous equation $fR'' + f'R' - gR = 0$. Also consider that R_a satisfies the homogeneous boundary condition of (B2a), and R_b that of (B2b), respectively. If $\varphi(r)$ is at least a piecewise continuous function of r, then, from the theory of integral equations,[1] the function

$$R(r) = \int_a^b G(r,z)\varphi(z)dz \qquad \text{(B3)}$$

is the complete solution of equation (B1) and it satisfies the given boundary conditions. The symbol G(r,z) in equation (B3) is a Green's function and it is constructed in the following manner:

$$G(r,z) = \begin{cases} -\frac{1}{\Gamma} R_b(z)R_a(r) & \text{for } r \leqq z \\ -\frac{1}{\Gamma} R_a(z)R_b(r) & \text{for } r \geqq z \end{cases} \qquad \text{(B4)}$$

where

$$\Gamma = f(z)[R_a(z)R_b'(z) - R_a'(z)R_b(z)] = \text{constant}$$

Now returning to the present case of equations (76) and (77), we see from the preceding analysis that the first step is to find the four linearly independent solutions, two for each equation, for the homogeneous equations (92) and (93). The solutions must be obtained in such a way that the two solutions for θ should satisfy the boundary conditions (83) and (86), respectively, and the two for m should satisfy (84) and (87), respectively. Note that the boundary conditions for the present case are all homogeneous.

[1]See references 20 and 21 for the complete treatment of the subject.

The general solutions of the homogeneous equations (92) and (93) are derived by the use of the known two solutions (94) and (95) as follows:

$$L_{\theta,n}(\eta) = C_1 H_{\theta,n}(\eta) \int_0^{\eta} \frac{dz}{[H_{\theta,n}(z)]^2 e^{Prz^2}} + C_2 H_{\theta,n}(\eta) \qquad (B5)$$

$$L_{m,n}(\eta) = C_3 H_{m,n}(\eta) \int_0^{\eta} \frac{dz}{[H_{m,n}(z)]^2 e^{Scz^2}} + C_4 H_{m,n}(\eta) \qquad (B6)$$

where C's are the constants of integration.

The appropriate application of the boundary conditions (83) through (87) to the above general solutions yields the four particular solutions (100) through (103) in such a way that each particular solution satisfies one of the boundary conditions. The expressions α_n represent the particular solutions of equation (92), and β_n represent those of equation (93). The subscripts w and ∞ refer to the boundary conditions they satisfy at the wall and at the outer edge of the boundary layer, respectively. The expressions $\alpha_{n,w}$ and $\alpha_{n,\infty}$, and $\beta_{n,w}$ and $\beta_{n,\infty}$, respectively, are linearly independent of each other and it can be proven easily by forming the proper Wronskians and showing that they do not vanish.

The Green's functions for the present case, $G_{\theta,n}(\eta,z)$ and $G_{m,n}(\eta,z)$, are constructed as equations (98) and (99) by use of the form (B4).

Finally, the complete solutions to the problem are derived, in accordance with equation (B3), as equations (96) and (97).

There is one special case for which a minor modification has to be made. The expression for C_m given by equation (104) becomes ∞ when $k_w = v_o/\sqrt{\nu} = 0$. Therefore, $\beta_{n,w}(\eta)$ for this case can not be obtained in the usual way. For this case, however, $m'_{n,w} = 0$ from (84), and it is seen that the solution $H_{m,n}(\eta)$ satisfies this boundary condition. Therefore, $H_{m,n}(\eta)$ is used instead of $\beta_{n,w}(\eta)$ when $k_w = v_o/\sqrt{\nu} = 0$.

The integrals, I, though straightforward, must be integrated numerically except for n = 1. The form of the homogeneous equations (92) and (93) becomes, when n = 1, identical to an equation derived in reference 22.

$$\frac{1}{Pr} R''(r) + \frac{r}{2} R'(r) - R(r) = 0$$

A 3 3 6

The two particular solutions are found in closed form, in the reference, to satisfy the boundary condition $R(-\infty) = 0$ and $R(\infty) = 0$, respectively. A little manipulation of these solutions yields the integrated expressions for $I_{\theta,1}(\eta)$ and $I_{m,1}(\eta)$ as:

$$I_{\theta,1}(\eta) = \int_0^{\eta} \frac{dz}{(1 + 2Prz^2)^2 e^{Prz^2}}$$

$$= \frac{1}{2}\left[\frac{\eta}{(1 + 2Pr\eta^2)^2 e^{Pr\eta^2}} + \sqrt{\frac{\pi}{4Pr}}\, \mathrm{erf}(\sqrt{Pr}\eta)\right]$$

and

$$I_{m,1}(\eta) = \int_0^{\eta} \frac{dz}{(1 + 2Scz^2)^2 e^{Scz^2}}$$

$$= \frac{1}{2}\left[\frac{\eta}{(1 + 2Sc\eta^2)^2} + \sqrt{\frac{\pi}{4Sc}}\, \mathrm{erf}(\sqrt{Sc}\eta)\right]$$

REFERENCES

1. Rosner, Daniel E.: Recent Advances in Convective Heat Transfer With Dissociation and Atom Recombination. Jet Propulsion, vol. 28, no. 7, July 1958, pp. 445-451.

2. Heims, Steve P.: Effect of Oxygen Recombination on One-Dimensional Flow at High Mach Numbers. NACA TN 4144, 1958.

3. Clarke, John F.: Energy Transfer Through a Dissociated Diatomic Gas in Couette Flow. Jour. Fluid Mech., vol. 4, pt. 5, Sept. 1958, pp. 441-465.

4. Penner, S. S.: Introduction to the Study of Chemical Reactions in Flow Systems. NATO-AGARD, Butterworths Scientific Pub., London, 1955.

5. Fay, J. A., and Riddell, F. R.: Theory of Stagnation Point Heat Transfer in Dissociated Air. Jour. Aero. Sci., vol. 25, no. 2, Feb. 1958, pp. 73-85, 121.

6. Camac, M., Camm, J., Feldman, S., Keck, J., and Petty, C.: Chemical Relaxation in Air, Oxygen, and Nitrogen. IAS Preprint 802, 1958.

7. Matthews, D. L.: Interferometric Measurement in the Shock Tube of the Dissociation Rate of Oxygen. The Physics of Fluids, American Institute of Physics, March-April 1959, pp. 170-178.

8. Adamson, T. C., Jr., Nicholls, J. A., and Sherman, P. M.: A Study of the Hypersonic Laminar Boundary Layer With Dissociation. Rep. 2606-6-T, Univ. of Michigan, Engr. Res. Institute, May 1957.

9. Broadwell, James E.: A Simple Model of the Non-Equilibrium Dissociation of a Gas in Couette and Boundary Layer Flows. Douglas Rep. SM-22888, Aug. 1957. (Also Jour. of Fluid Mech., vol. 4, pt. 2, June 1958, pp. 113-139)

10. Liepmann, H. W., and Bleviss, Z. O.: The Effects of Dissociation and Ionization on Compressible Couette Flow. Douglas Rep. SM-19831, May 1956.

11. Chambré, P. L., and Acrivos, A.: On Chemical Surface Reactions in Laminar Boundary Layer Flows. Jour. Appl. Phys., vol. 27, no. 11, Nov. 1956, pp. 1322-1328.

12. Goulard, Robert J.: On Catalytic Recombination Rates in Hypersonic Stagnation Heat Transfer. ARS Preprint 544-57, 1957. (Also Jet Propulsion, vol. 28, no. 11, Nov. 1958, pp. 737-745)

A 3 3 6

13. Rosner, Daniel E.: Chemically Frozen Boundary Layers With Catalytic Surface Reaction. Jour. Aero/Space Sci., vol. 26, no. 5, May 1959, pp. 281-286.

14. Eckert, E. R. G., and Schneider, P. J.: Mass-Transfer Cooling in High-Speed Laminar Couette Flow. Tech. Rep. No. 12, Univ. of Minnesota, April 1957.

15. Knuth, Eldon L.: Compressible Couette Flow With Diffusion of a Reactive Gas From a Decomposing Wall. Preprints of Papers, Heat Transfer and Fluid Mechanics Institute, Univ. of Calif., Berkeley, Calif., June 19-21, 1958, pp. 104-113.

16. Hartnett, J. P., and Eckert, E. R. G.: Mass Transfer Cooling With Combustion in a Laminar Boundary Layer. Preprints of Papers, Heat Transfer and Fluid Mechanics Institute, Univ. of Calif., Berkeley, Calif., June 19-21, 1958, pp. 54-68.

17. Emmons, H. W.: The Film Combustion of Liquid Fuel. Interim TR 6, 1953, Harvard Univ., Div. of Appl. Sci. (Also Zeitschrift Für Angewandte Mathematic und Mechanik, Band 36, Jan. 1956, pp. 60-71)

18. Feldman, Saul: Hypersonic Gas Dynamic Charts for Equilibrium Air. Res. Rep. No. 12, AVCO Research Laboratory, Jan. 1957.

19. Chung, Paul M.: Shielding Stagnation Surfaces of Finite Catalytic Activity by Air Injection in Hypersonic Flight. NASA TN D-27, 1959.

20. Lovitt, W. V.: Linear Integral Equations. Dover Publications, Inc., New York, 1950, Chap. 6.

21. Courant, R., and Hilbert, D.: Methods of Mathematical Physics. Interscience Publishers, Inc., vol. 1, New York, 1953, pp. 351-358.

22. Marble, Frank E., and Adamson, Thomas C., Jr.: Ignition and Combustion in a Laminar Mixing Zone. Selected Combustion Problems. NATO-AGARD, Butterworths Scientific Pub., London, 1954, pp. 111-131.

A
3
3
6

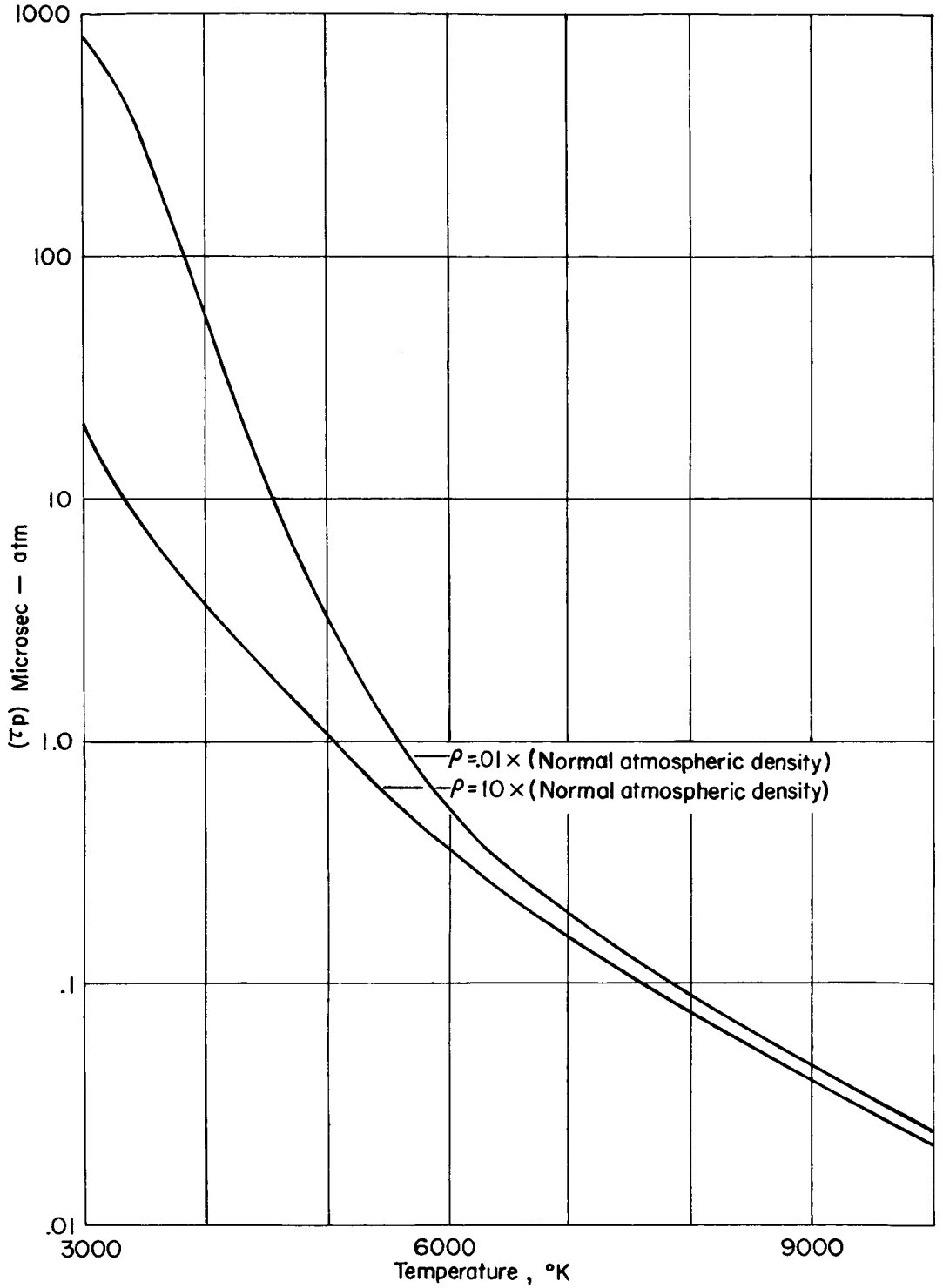

Figure 1.- Relaxation time for oxygen dissociation and recombination (obtained directly from ref. 2).

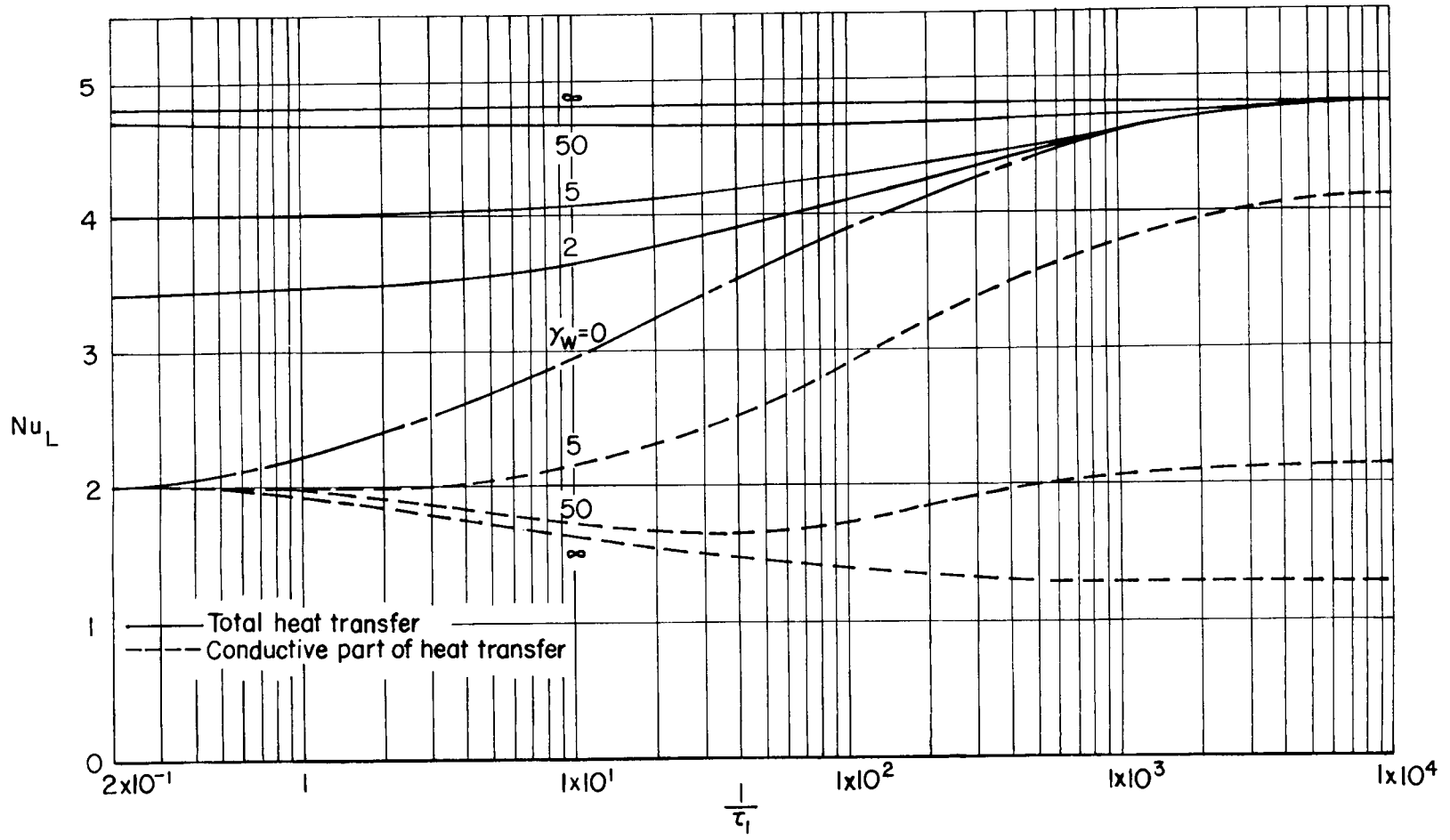

(a) $\delta = 0$

Figure 2.- Heat-transfer variation for Couette flow.

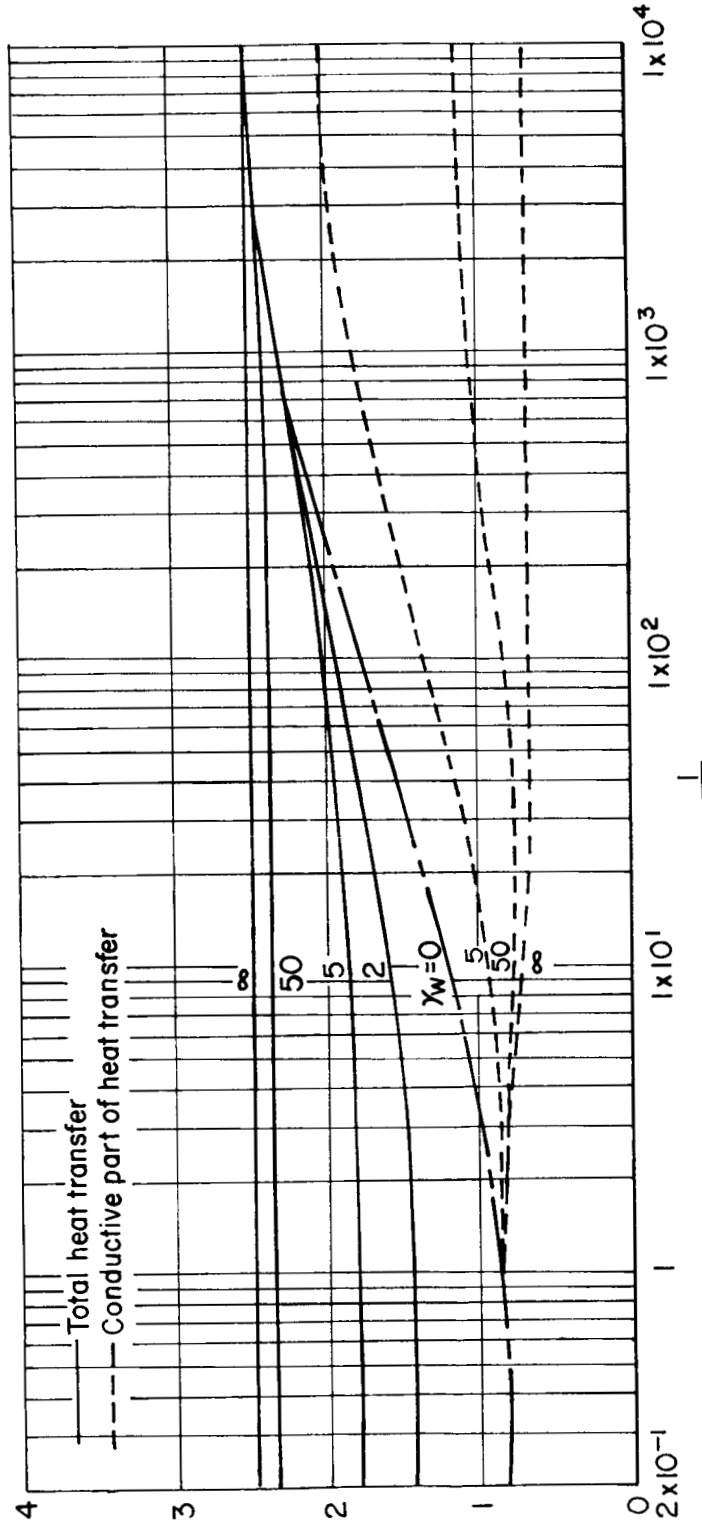

(b) $\delta = 2$

Figure 2.- Concluded.

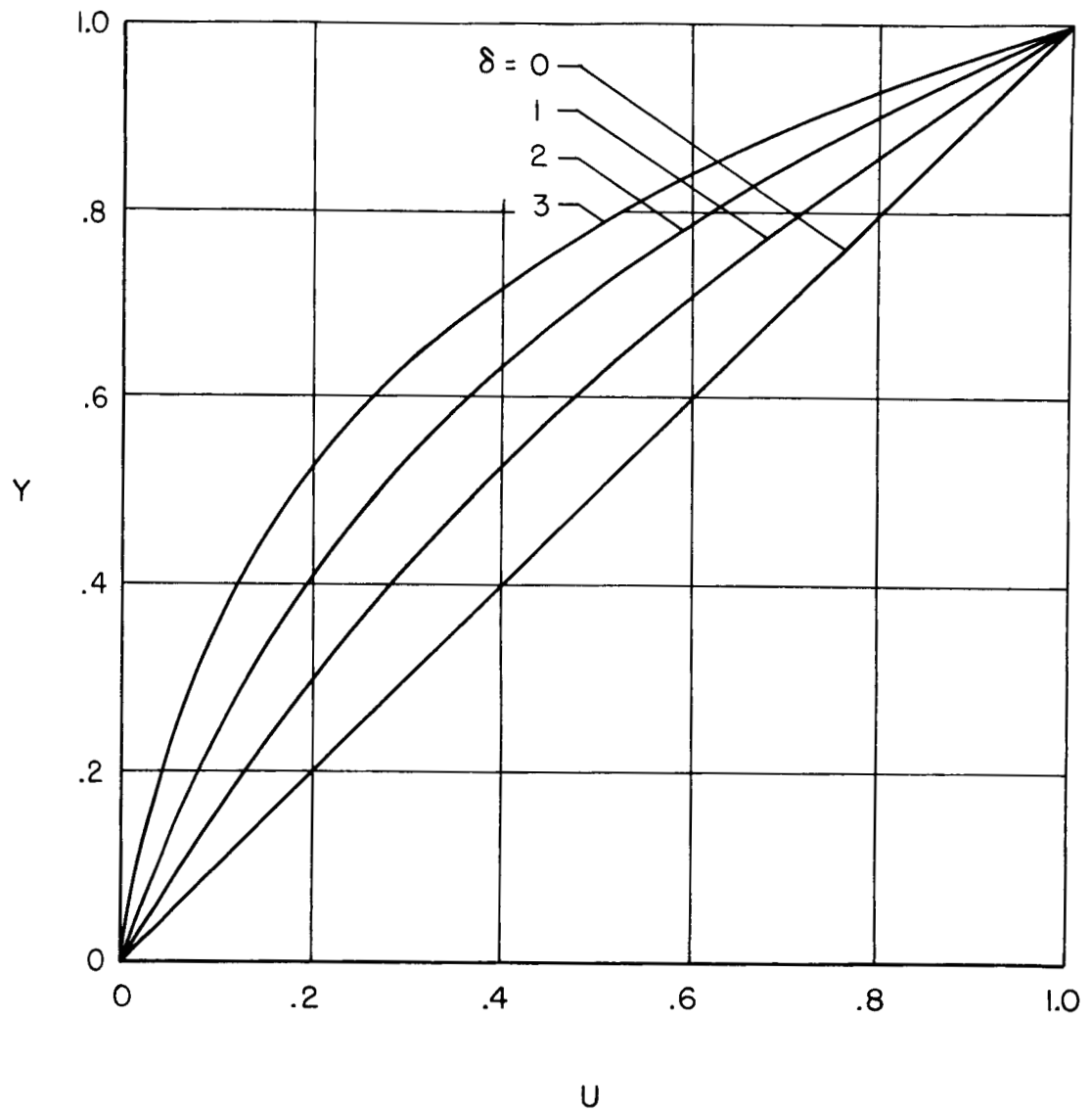

Figure 3.- Velocity profiles for Couette flow.

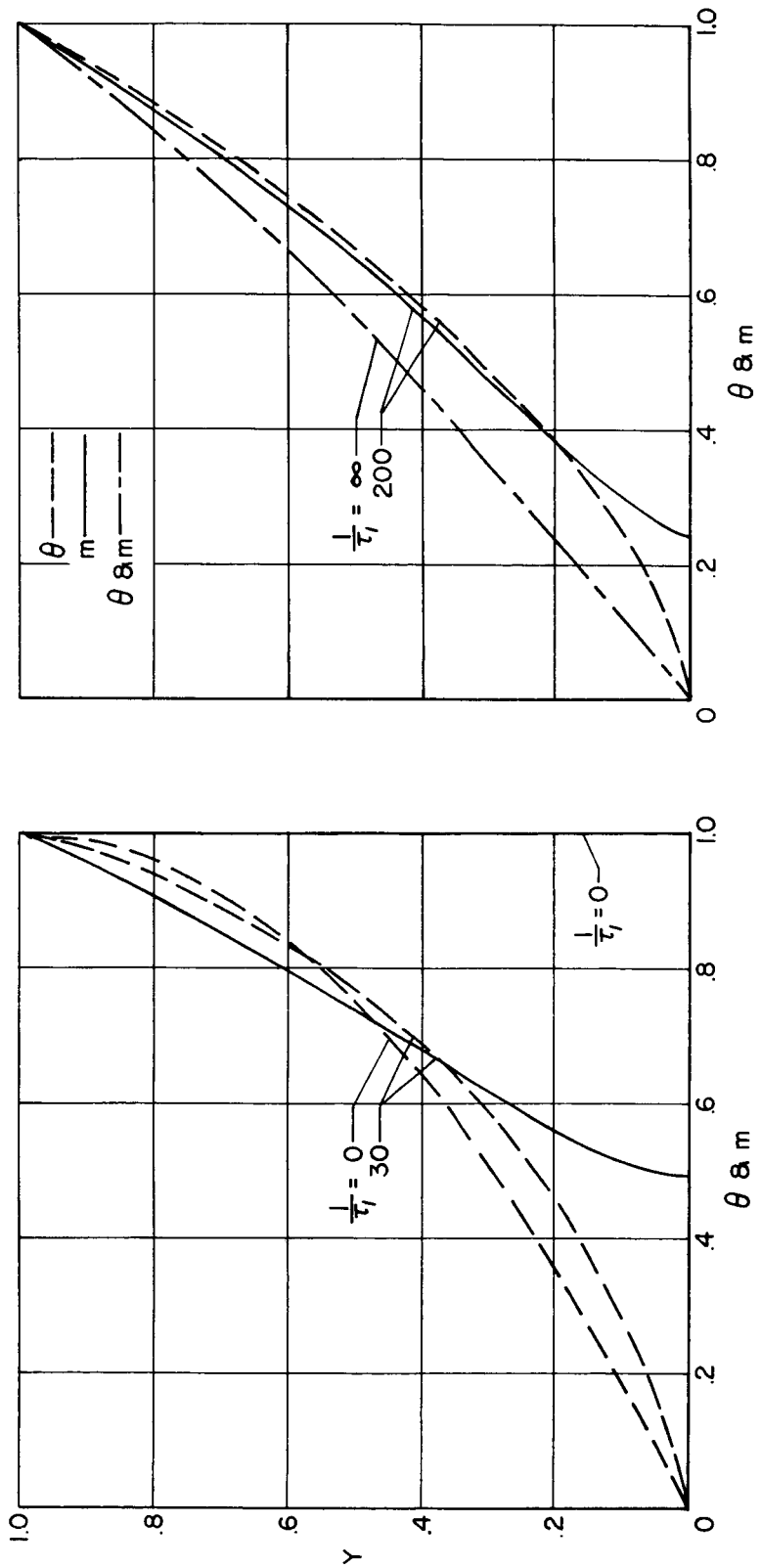

Figure 4.- Dimensionless temperature and atom-concentration profiles for $\delta = 0$; $\gamma_w = 0$.

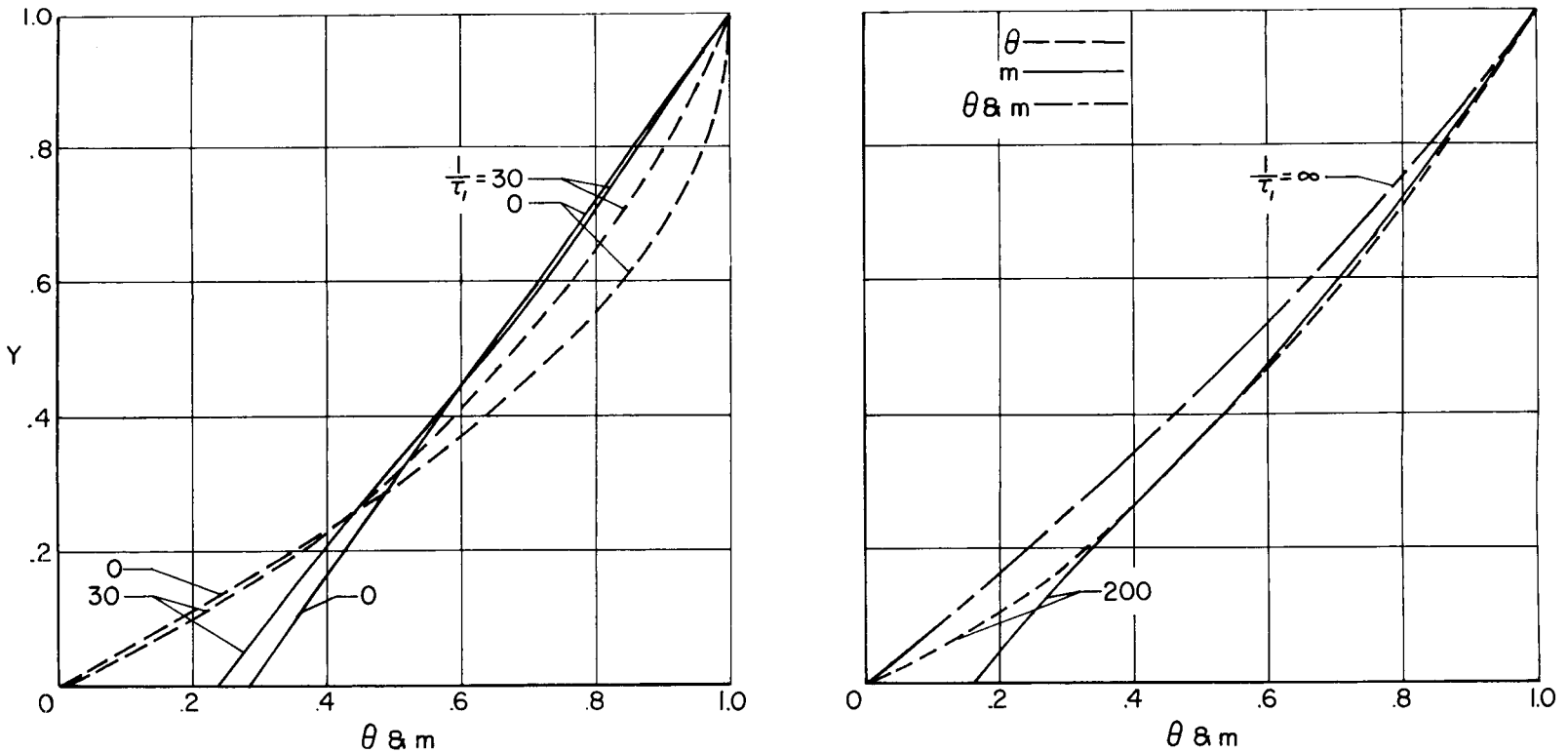

Figure 5.- Dimensionless temperature and atom-concentration profiles for $\delta = 0$; $\gamma_w = 5$.

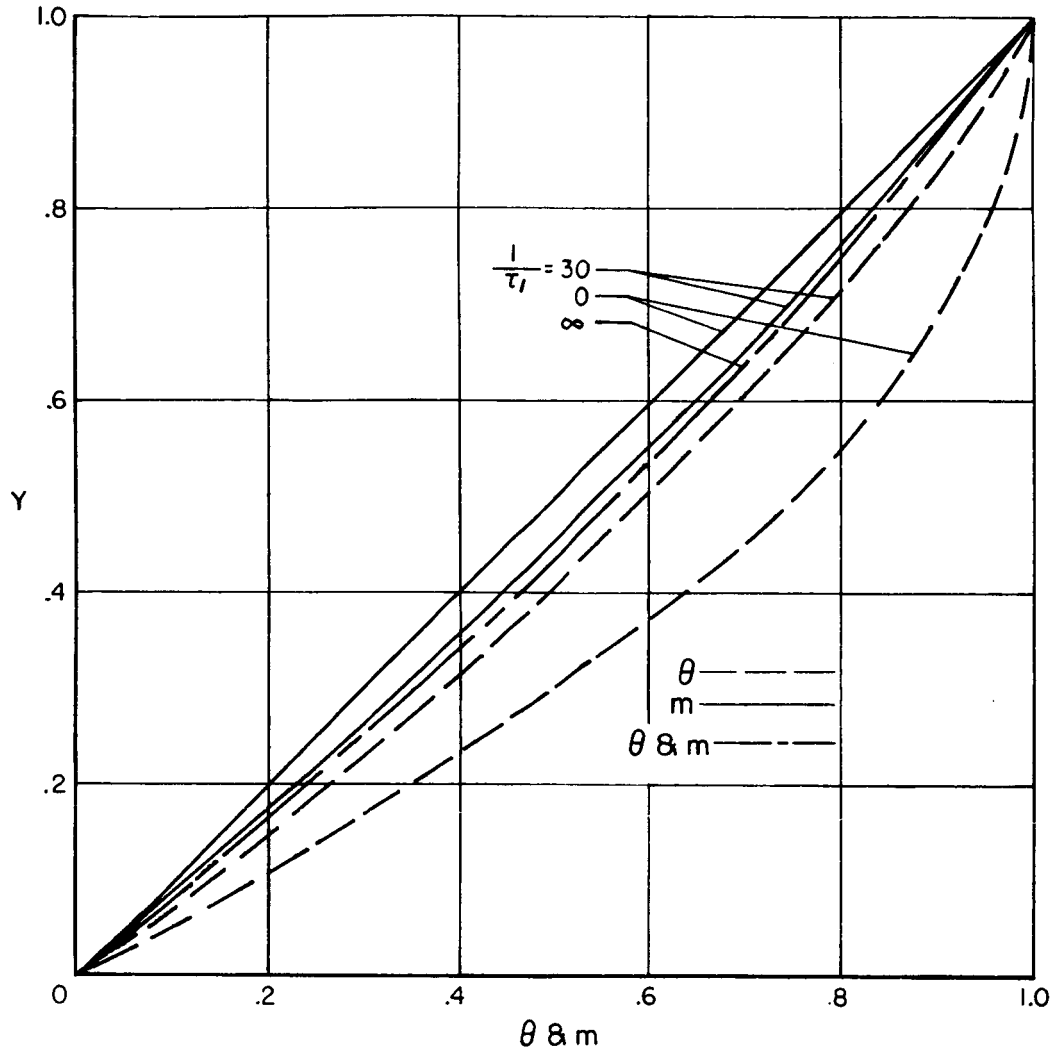

Figure 6.- Dimensionless temperature and atom-concentration profiles for $\delta = 0$; $\gamma_w = \infty$.

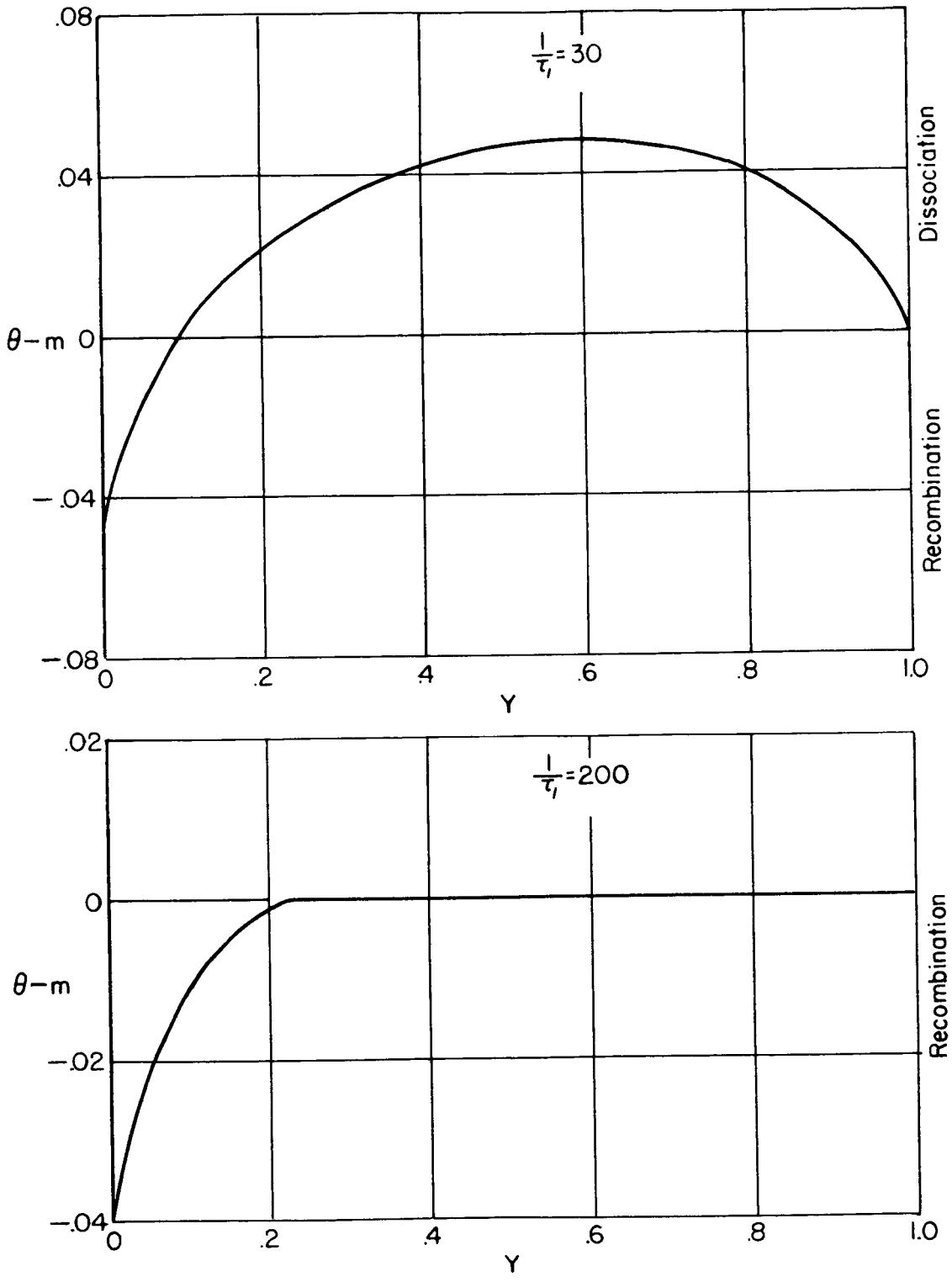

Figure 7.- Gas-phase reaction rate for $\gamma_w = 50$; $\delta = 0$.

A
3
3
6

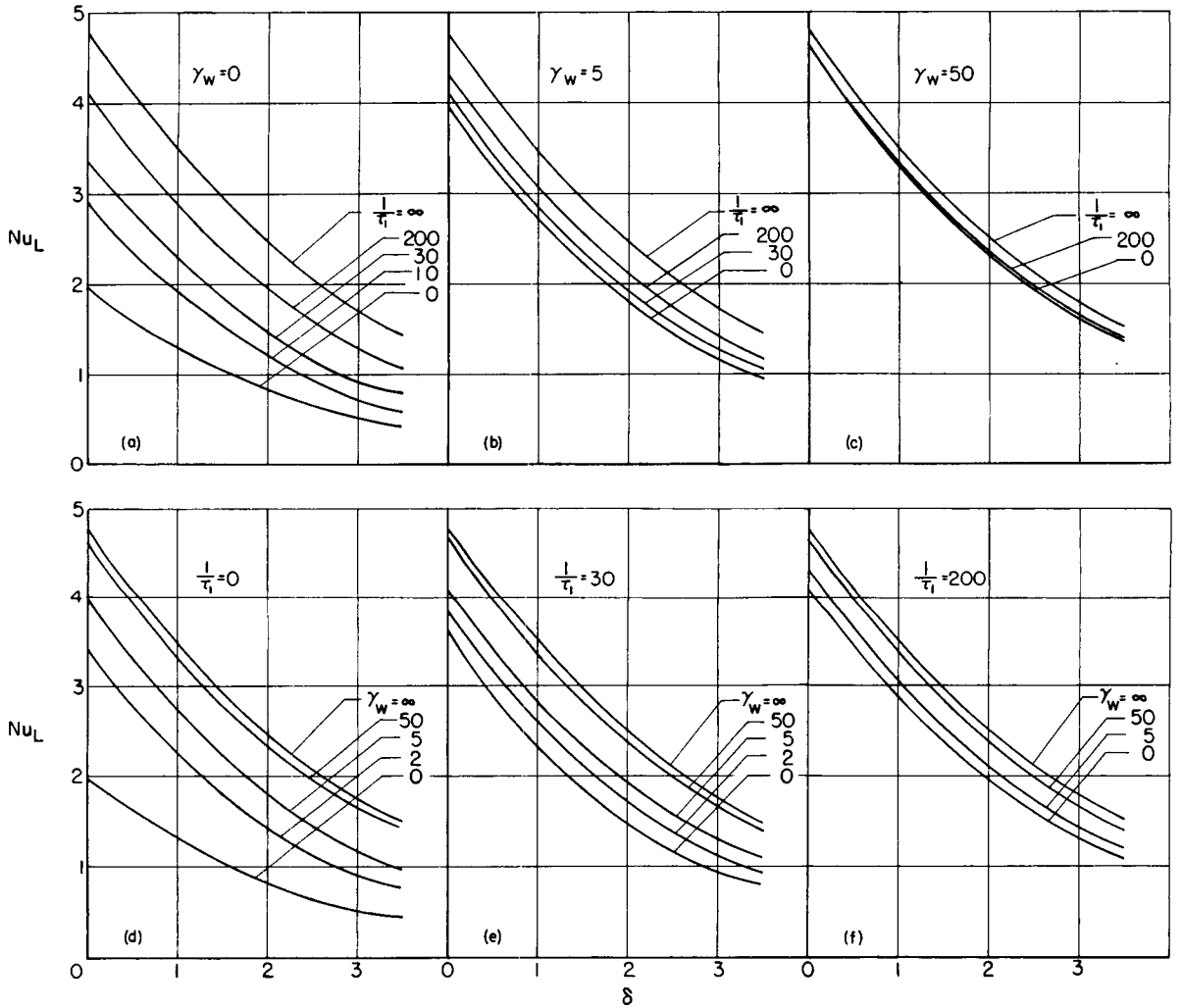

Figure 8.- Variation of heat transfer with respect to specific gas-phase and surface reaction rates and with respect to fluid-injection rate.

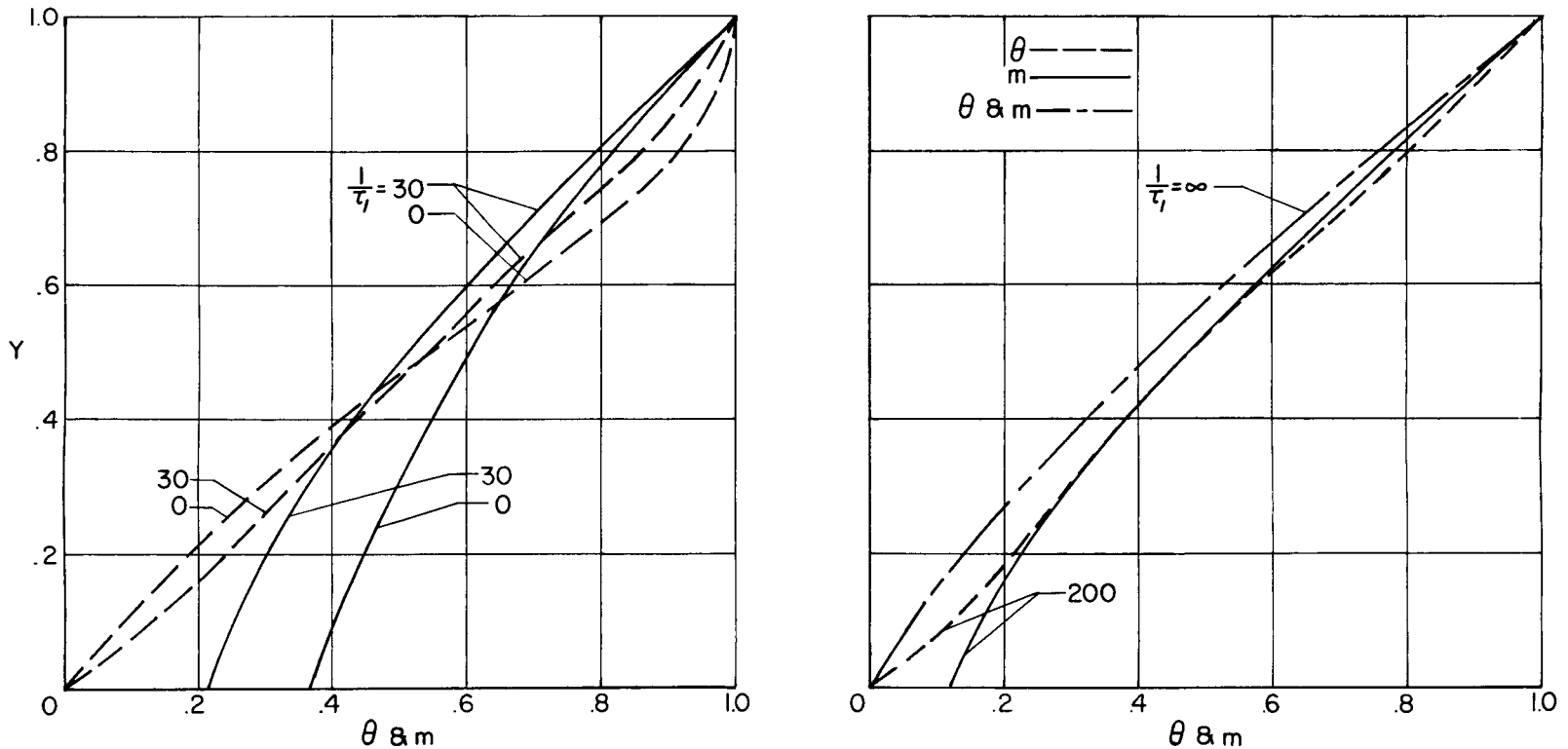

Figure 9.- Dimensionless temperature and atom-concentration profiles for $\delta = 2$; $\gamma_w = 0$.

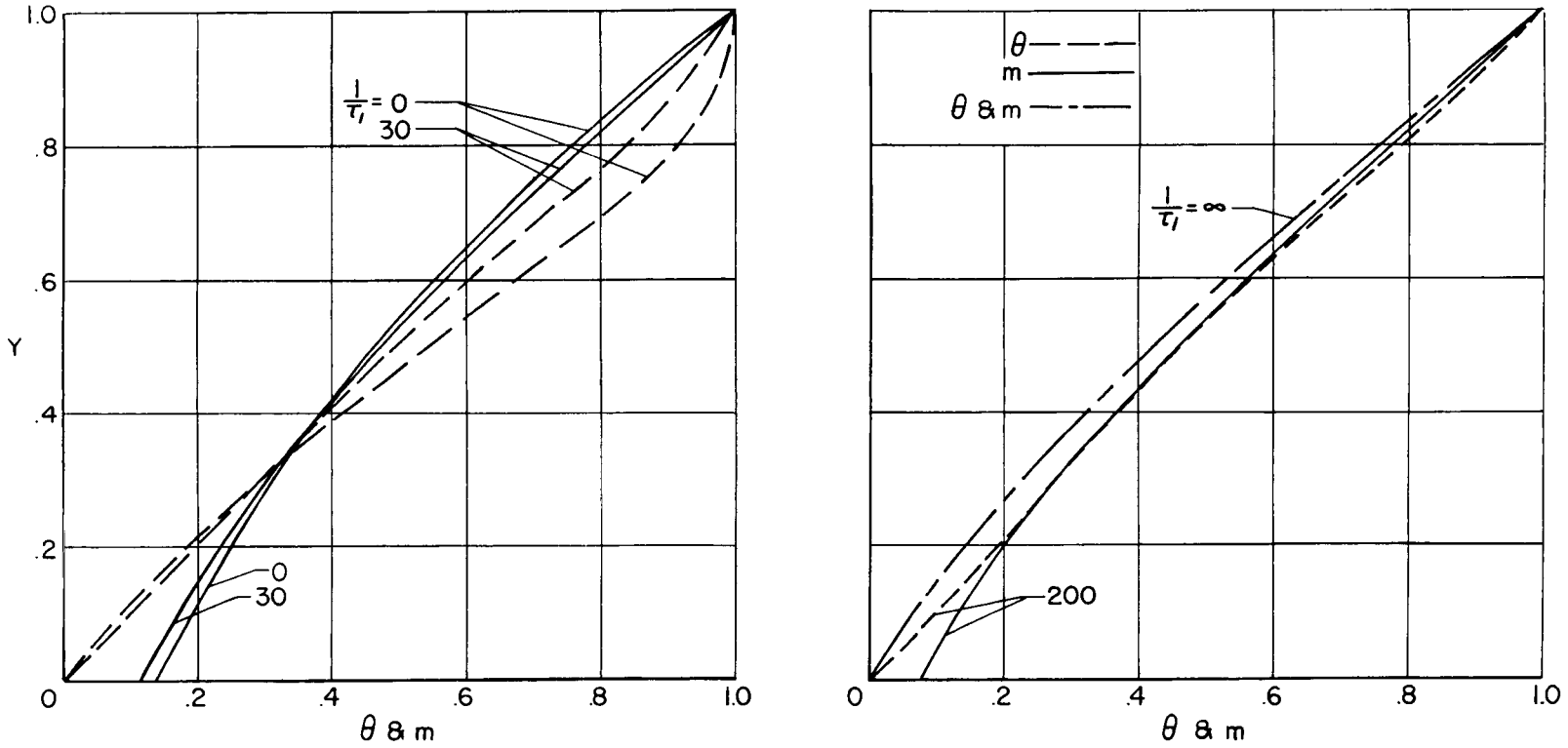

Figure 10.- Dimensionless temperature and atom-concentration profiles for $\delta = 2$; $\gamma_w = 5$.

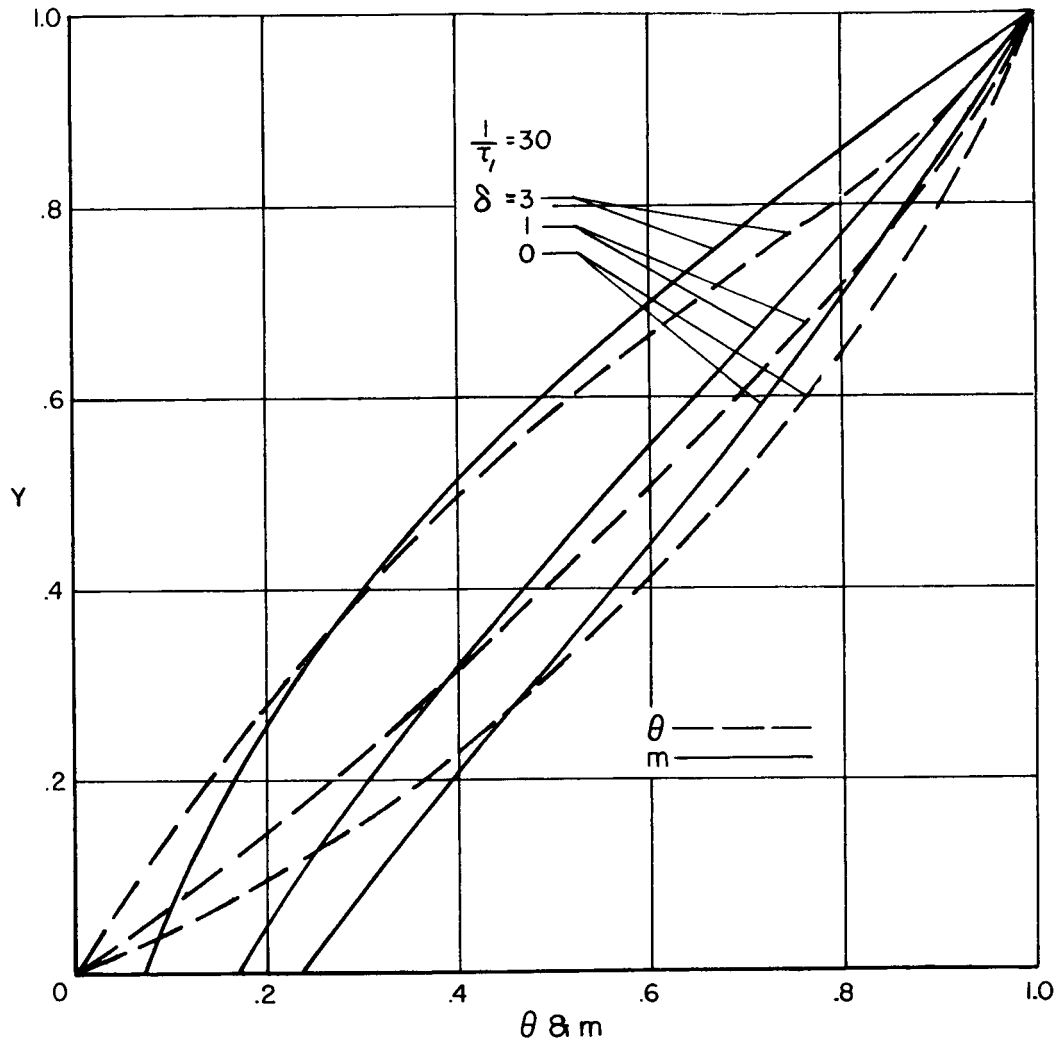

Figure 11.- Typical variation of dimensionless temperature and atom-concentration profiles with respect to injection rate.

A
3
3
6

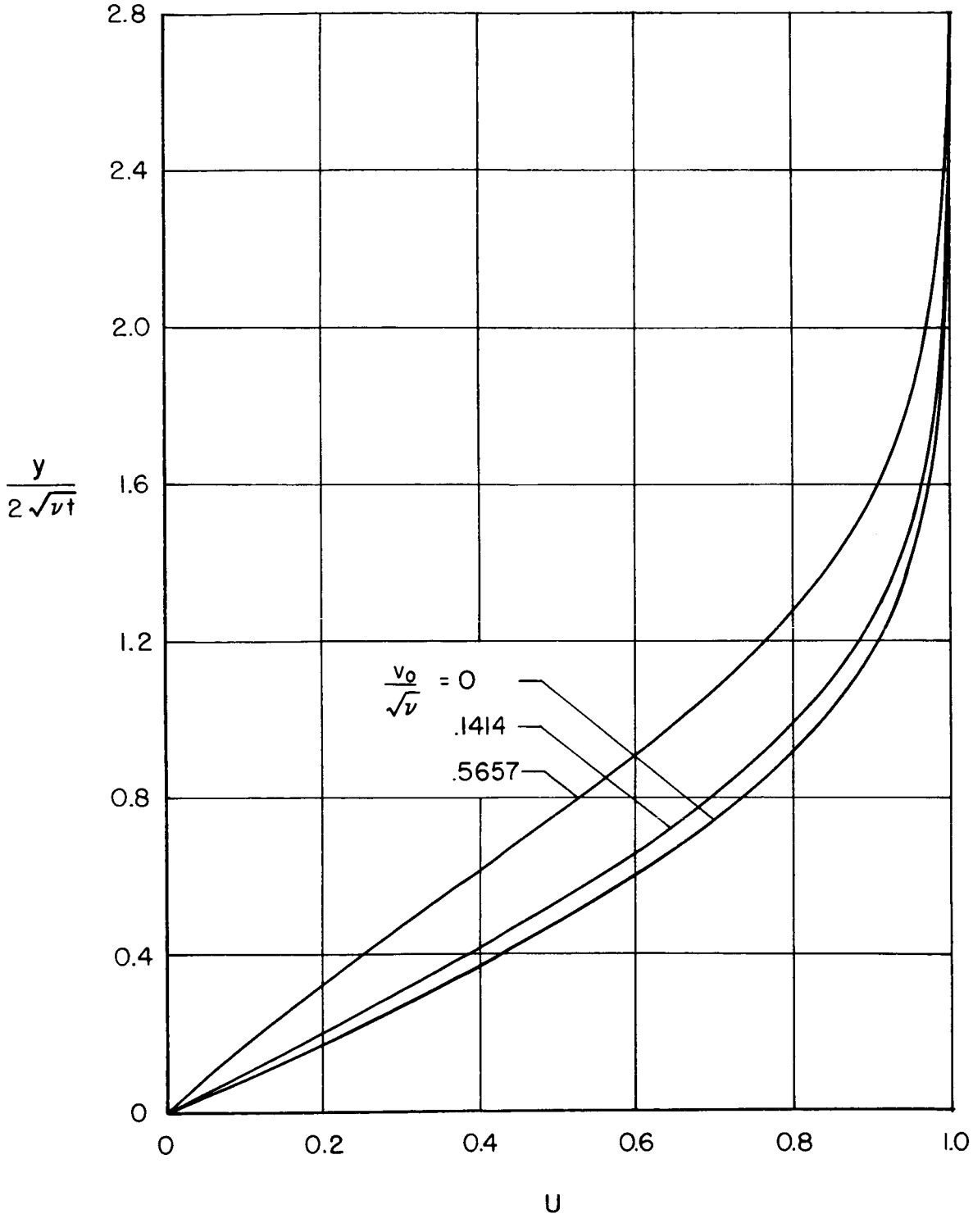

Figure 12.- Velocity profiles for Rayleigh's problem.

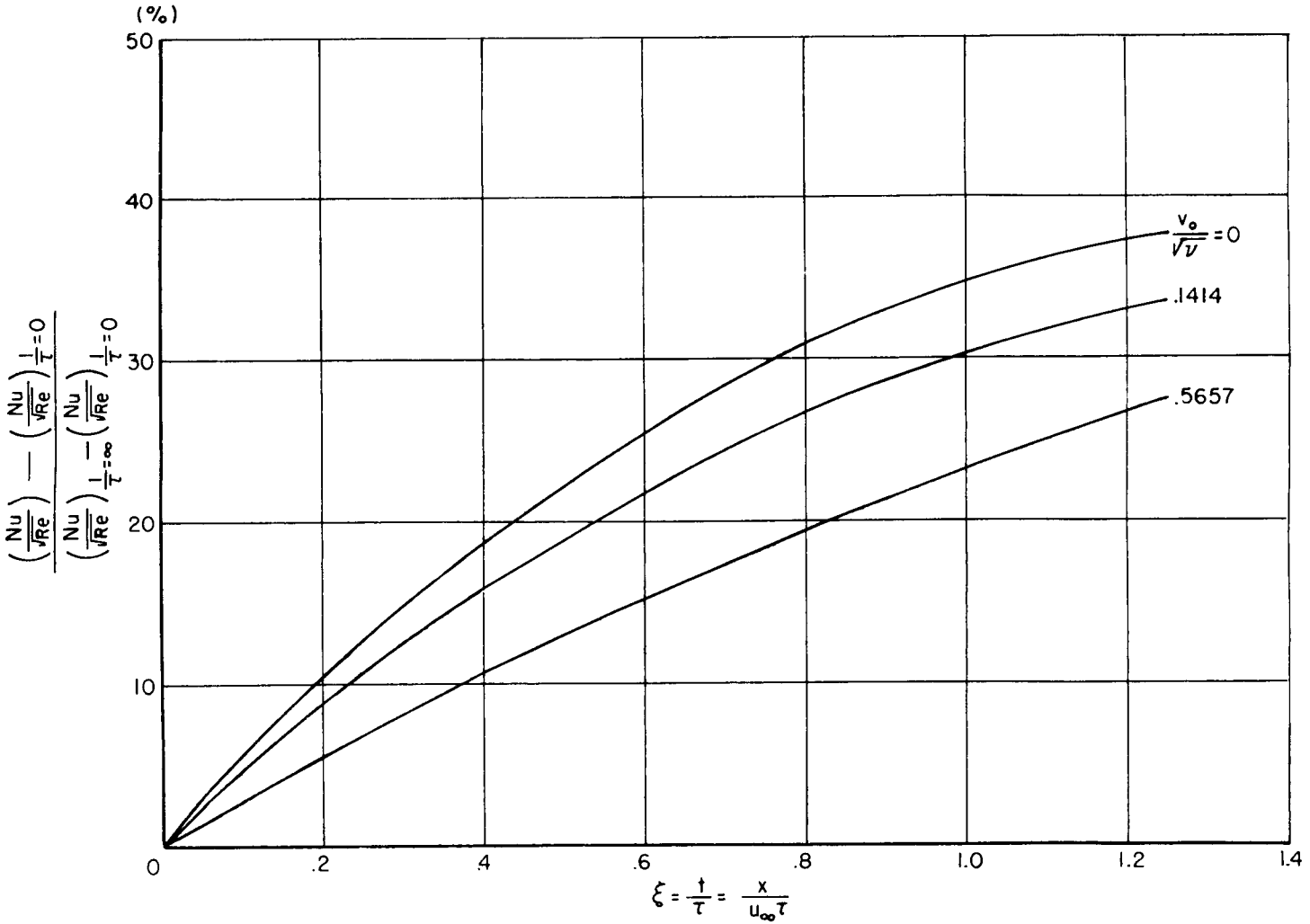

Figure 13.- Variation of heat transfer for boundary-layer flow with respect to ξ and injection rate.

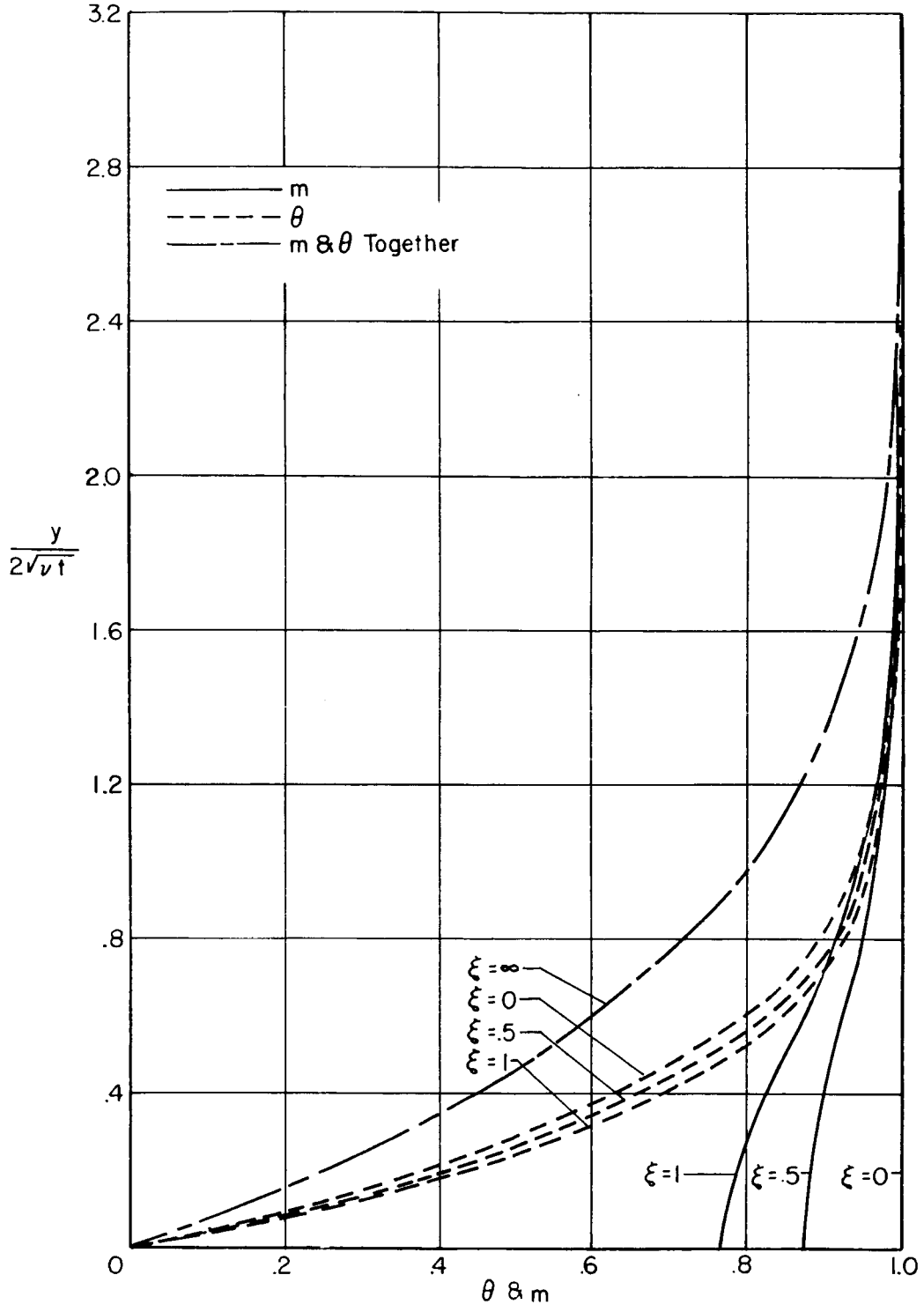

Figure 14.- Dimensionless temperature and atom-concentration profiles for boundary-layer flow with $(v_o/\sqrt{\nu}) = 0$.

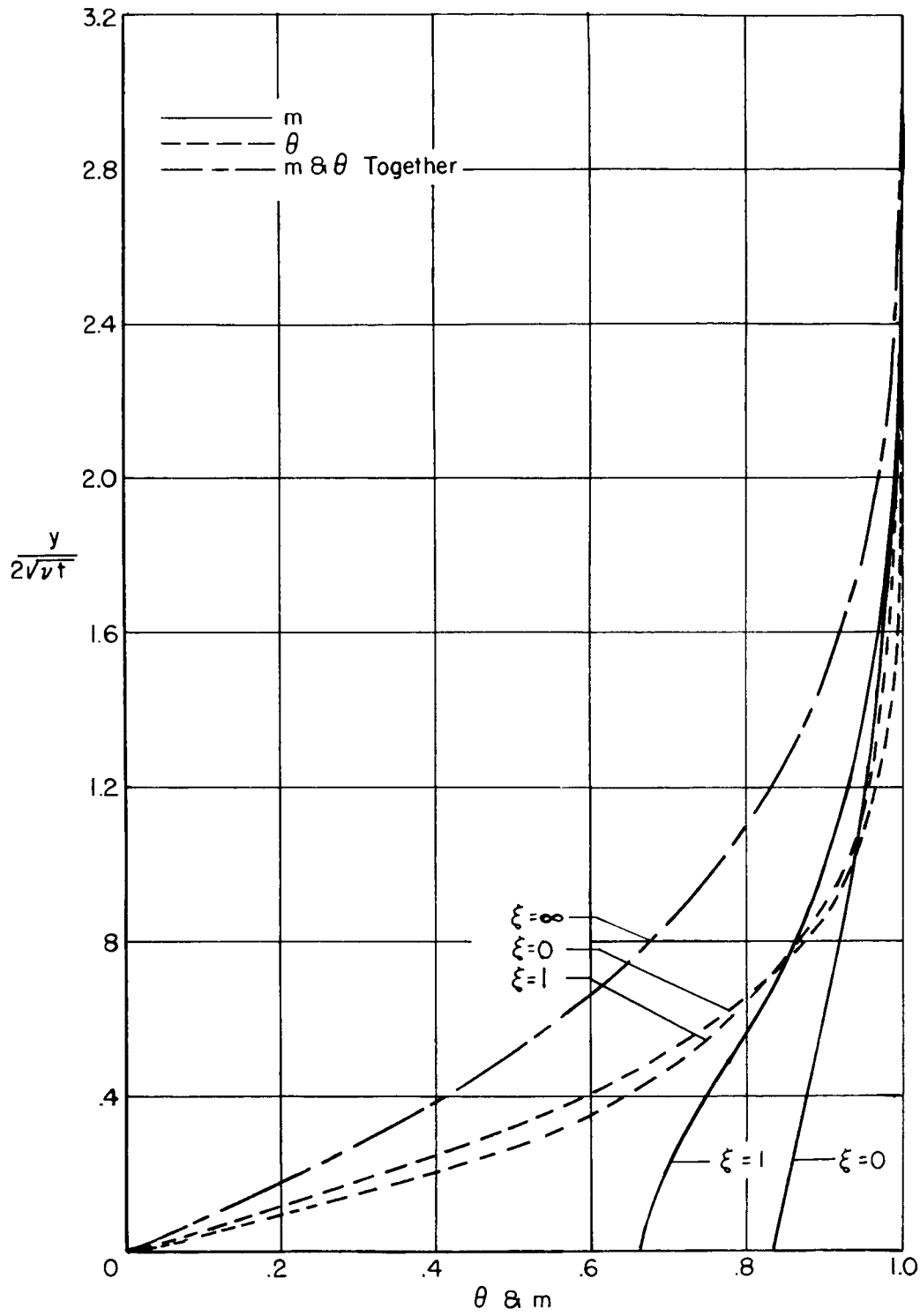

Figure 15.- Dimensionless temperature and atom-concentration profiles for boundary-layer flow with $(v_o/\sqrt{\nu}) = 0.1414$.

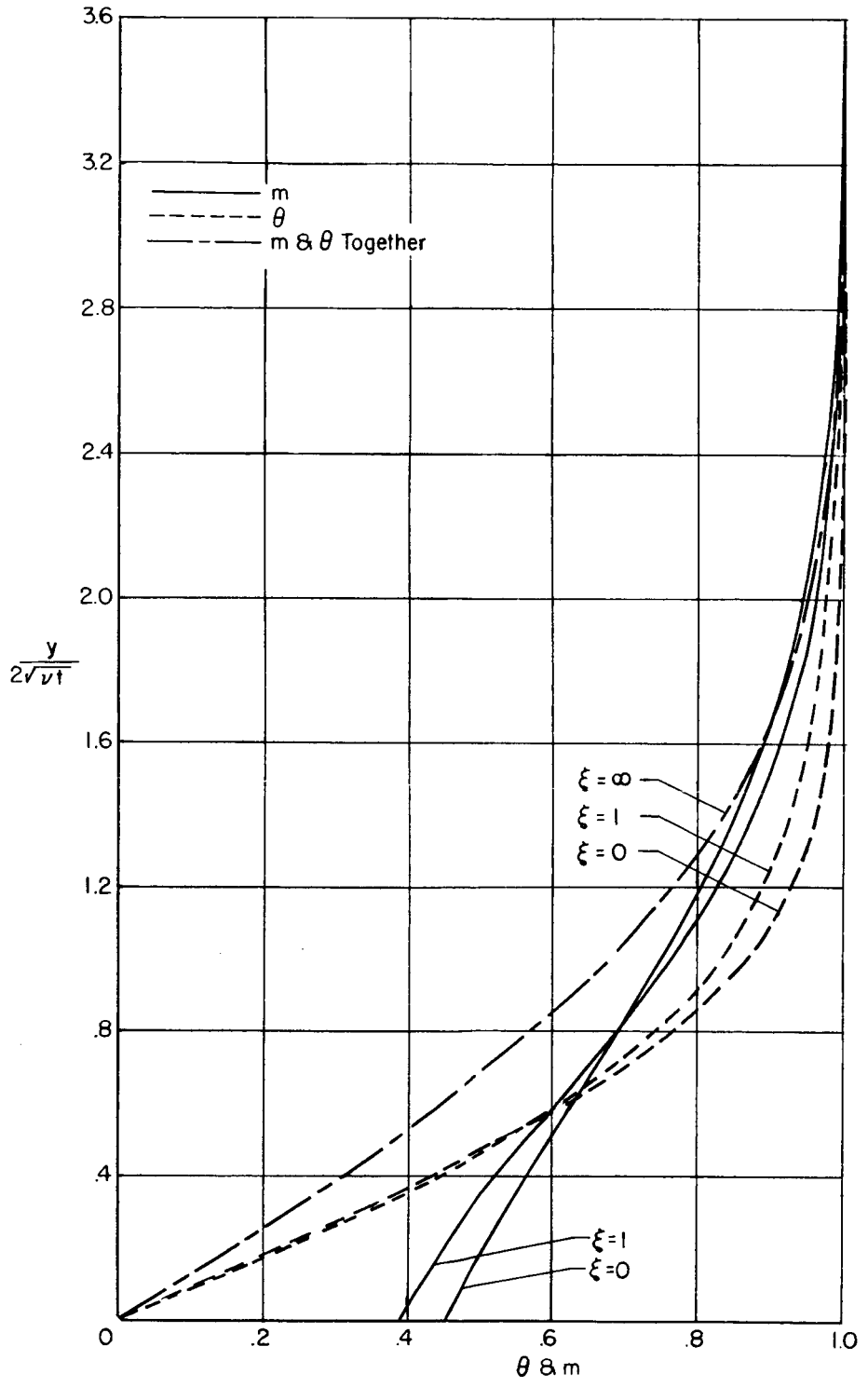

Figure 16.- Dimensionless temperature and atom-concentration profiles for boundary-layer flow with $(v_o/\sqrt{\nu}) = 0.5657$.